SEMI-ANNUAL TECHNICAL REPORT

Grant Number:	NASA Research Grant No. NSG-7610
Name of Contractor:	California Institute of Technology Pasadena, California 91125
Principal Investigator:	Don L. Anderson Seismological Laboratory, 252-21 California Institute of Technology Pasadena, California 91125
Co-Investigators:	Bradford H. Hager Hiroo Kanamori Seismological Laboratory 252-21 California Institute of Technology Pasadena, California 91125
NASA Technical Officer:	J. A. Vitale - Code ETD-6 NASA Washington, D. C. 20545
Title:	Fundamental Studies in Geodynamics
Period of Grant:	1 August 1980 - 31 July 1981
Period of Report:	1 February 1981 - 31 July 1981

Introduction

Research in fundamental studies in geodynamics has continued in a number of fields including seismic observations and analysis, synthesis of geochemical data, theoretical investigation of geoid anomalies, extensive numerical experiments in a number of geodynamical contexts, and a new field--seismic volcanology.

Summaries of work in progress or completed during this report period are given below. Abstracts of publications submitted from work in progress during this report period are attached as an appendix.

Analysis of Long-Period Surface Waves Excited by Mt. St. Helens Eruption on May 18, 1980 --Terrestrial Monopole?

The eruption of Mt. St. Helens on May 18, 1980 excited long-period seismic surface waves which were recorded clearly by the IDA, SRO and ASRO stations. Some examples are shown in Figure 1a, b and c. In general, Love waves are larger than Rayleigh waves. The spectra of these surface waves are computed and equalized to the source. Figure 2 shows the amplitude spectra of Love and Rayleigh waves as a function of azimuth around the source. Both Love and Rayleigh waves show a two-lobed radiation pattern with a nodal direction in about N10^{o}E and E10^{o}S for Love and Rayleigh waves respectively.

These radiation patterns have been interpreted by Prof. Kanamori and Jeff Given using normal mode theory. It can be shown that no double-couple source can produce the radiation patterns shown in Figure 2. The radiation patterns for a single horizontal force, a single vertical force and an isotropic source are computed and are

schematically shown in Figure 3. Comparison of Figure 3 with Figure 2 immediately suggests that an almost horizontal single force in either N10°E or S10°W direction is a good representation of the source. Kanamori and Given performed a detailed inversion of the source spectra at periods of 100, 120, 150, 200 and 256 sec to determine the geometry of the source. On the basis of this inversion they conclude that the force is nearly horizontal (with E15° from the horizontal) and its horizontal projection is in the direction S5°W.

By using the source spectrum and the synthetic seismograms they determined the time history of the source. They assumed the source time function in the form:

$$s(t) = 1/2(1-\cos\tfrac{t}{\tau}\pi)) \qquad 0 \leq t \leq 2\tau$$

$$= 0 \qquad t \geq 2\tau$$

and computed synthetic seismograms for various values of τ (Figure 4). Comparison of the synthetics with the observed records indicates that τ = 75 sec is appropriate. From the amplitude spectrum, the peak value of the force is determined to be 10^{18} dyne.

This result provides important constraints on the mechanics of volcanic eruption. They plan to present this result at the coming Fall AGU meeting in San Francisco, and a full paper which describes the details of the analysis is now in preparation.

Upper mantle anisotropy

There is a growing body of evidence that much of the mantle is anisotropic with respect to the propagation of seismic waves. Professor Anderson, working with Professor Dziewonski of Harvard and with students at the Seismological Laboratory, is investigating this phenomenon.

The presence of anisotropy is not only of theoretical interest. If the upper mantle is, in fact, anisotropic then isotropic inversion of seismic data will result in erroneous structures because of improper parameterization. Such important geodynamical problems as the presence and nature of a low-velocity zone and the depth extent of differences between oceans and continents depend critically on the validity of the assumption of isotropy.

Since intrinsic anisotropy requires both anisotropic crystals and preferred orientation, the anisotropy of the mantle contains information both about the mineralogy and the flow pattern in the mantle. For example, olivine, the most abundant upper mantle mineral, is extremely anisotropic for both P-wave and S-wave propagation. It apparently is easily oriented by the ambient stress or flow field. Olivine-rich outcrops show a consistent preferred orientation over large areas. In general, the seismically fast axes are in the plane of the flow with the a-axis, the fastest direction, pointing in the direction of flow. The b-axis, the minimum velocity direction, is generally normal to the flow plane. On a global basis, Anderson and Dziewonski find that the average anisotropy in the upper 200 km of the mantle is that which would result from the horizontal shearing associated with plate motion. There is evidence that under ridges, the sense of anisotropy is reversed,

consistent with upwelling flow there.

Dynamic calculations of geoid anomalies

Geoid anomalies are usually interpreted in terms of density contrasts buried in a rigid Earth. Theoretical work by graduate student Mark Richards and Professor Hager shows that for a more realistic viscous earth, density contrasts cause flow and stresses which deform the top surface and any internal boundaries, as illustrated in Figure 5. This boundary deformation has an important effect on the total geoid anomaly - in fact, for a uniform viscosity earth, a negative geoid anomaly results from a positive density contrast. The total anomaly can be an order of magnitude larger than the anomaly from the density contrast alone, as shown in Figure 6. This is because the stresses causing deformation of the surface fall off less rapidly with depth than the potential from the density contrast.

These calculations have been generalized to include an earth with varying viscosity and with chemical layering. The magnitude and sign of the total anomaly is a strong function of the properties of the layers.

Finite element code for geodynamics applications

The rheology of the mantle is complicated, as is the geometry in many situations of interest in geodynamics. Numerical experiments with realistic geometries and rheologies are essential to test hypotheses and to give insight into the physics of geologic processes. The finite element technique is best suited for application to geodynamics problems.

Professor Hager, along with Dr. Arthur Raefsky, Visiting Associate, has spent a substantial portion of this period developing a

specialized finite element code tailored for solution of problems of interest in geodynamics. This code, except for cosmetic revisions, is complete and a manual for its use is being written. Much of the numerical work reported below was done using this code.

Ridge Processes

Two very important observations are that oceanic crustal thickness is independent of spreading rate and that the entire crustal section is formed completely essentially at the ridge axis. The first observation has been interpreted in terms of a passive model of a ridge, in which upwelling under ridges fills in the void left by spreading plates. In this model, isothermal upwelling beneath ridges is a passive response to, rather than a driving mechanism for plate motions.

Professor Hager has calculated the flow pattern beneath ridges according to the assumptions of the passive model and using a realistic nonNewtonian rheology. Streamlines are shown in Figure 7. These streamlines are more widely spaced beneath ridges than they are beneath plates, indicating that upwelling occurs over a wide region. Melt will rise vertically, so this passive model is inconsistent with the requirement that the crust be formed at the ridge axis.

Professor Anderson arrived at the conclusion that ridges are active, not passive, from geochemical considerations. In his model, diapirs of picritic melt rise from an olivine-eclogite layer at a depth of 220 km.

It is essential in Anderson's model that the diapirs rise rapidly enough that crystals not settle. He argued previously that the effects of nonNewtonian rheology will lead to rapid ascent. Hager and Raefsky

have computed more detailed finite element models to quantify the effect. Ascent velocities of meters/day are to be expected.

The flow pattern within a rising diapir will tend to keep crystals from settling. This flow, as well as the ascent velocity of a diapir, depends on its shape. Graduate student Cathryn Allen has determined using numerical experiments that diapirs evolve into spheres. She is in the process of determining crystal settling criteria for rising diapirs.

Earthquake migration and rheology of the asthenosphere

Four large earthquakes occurred in a seismic gap of category 2 (McCann et al., 1979) near the Loyalty Is. in the New Hebrides. At 3:25 on October 24, 1980, an event with M_S = 6.7 initiated the sequence. Three events, M_S = 6.7, 7.2, and 6.5 followed this event on the next day.

Graduate student John Vidale and Professor Kanamori investigated this sequence by using the PDE data, first-motion data from WWSSN records, and long-period surface waves recorded by IDA, SRO, and ASRO stations. The first-motion data constrained one of the nodal planes. With this constraint, inversion of Rayleigh and Love-wave spectra at 256 seconds determined the other nodal plane. The mechanisms of all four events were almost pure thrust on a plane dipping 20° and striking parallel to the local strike of the New Hebrides trench. The first-day aftershocks indicate an initial rupture zone of about 2,000 km^2 which is consistent with the estimated seismic moment of 3×10^{27} dyne-cm. This cluster of activity is shown in Figure 8. During the next two days, the aftershock activity expanded to an area of 110,000 to 20,000 km^2 in the directions both along and perpendicular to the trench. The expanded

zone of seismicity is also shown in Figure 8. This pattern suggests that the initial rupture zone represented a zone of increased strength (i.e. asperity), and the stress change due to failure of this asperity subsequently migrated outward. The events on the west side of the trench, the largest of which appears to have been a normal event from its first motions, were almost undoubtably triggered by the thrust events. Two similar thrust sequences in the New Hebrides have caused similar aftershock normal events.

We are using this data set, one of the cleanest of its kind, to investigate the dyanamic response of the lithosphere to stress loads from large thrust events. We expect to be able to place tighter constraints on the coupling between the lithosphere and asthenosphere and on the rheology of the asthenosphere. This data should provide a useful test of the rheological model previously developed under this grant by Anderson and Minster.

Seismic coupling at subduction zones

Graduate student Larry Ruff and Professor Kanamori have previously shown that M_w, the maximum characteristic size of earthquakes at subduction zones, is well correlated with convergence rate and plate age (Figure 9). In an attempt to understand the physics governing this correlation, they have examined earthquake source parameters for representative events in the northern Pacific.

They find that the maximum earthquake size is governed by the asperity distribution on the fault plane. Large events are characterized by rupture of large asperities, while smaller events are characterized by rupture of multiple smaller asperities (see Figure 10).

It is likely that asperity size is related to the state of stress in the slab, which is in turn related to slab trajectory. Graduate student Jia Jung Zhang is studying the relation between slab trajectory and stress in slabs using finite element models constrained by observed gravity, topography, and slab trajectory.

The global mantle flow pattern must influence slab trajectory. Professor Hager has computed pressures from the global return flow for a variety of models. He finds that for models with flow extending throughout the mantle, maximum earthquake size correlates well with this pressure field.

Seismicity and composition of volcanic rocks in island arcs

Plate subduction is generally considered to be the ultimate cause of large earthquakes and volcanism at island arcs. The activity of large earthquakes can be related to various parameters of plate subduction. Here we measure seismic activity by the magnitude M_w of the largest characteristic earthquake for each subduction zone.

There is a general correlation between M_w and plate convergence rate V, and M_w and the age of the subducting plates, T, as shown in Figure 9. This correlation is not unexpected because of M_w reflects the strength of inter-plate coupling, and V and 1/T are considered to be proportional to the strength of plate coupling (Ruff and Kanamori, 1980). On the other hand, various parameters for arc volcanic rocks have been associated with other characteristic features of island arcs. Among them are the ratio CA/TH (Cal-Alkali Series/Tholeiitic Series) (Miyashiro, 1974), Silica Index Θ (Sugimura, 1968), Alkali (K_2O, Na_2O etc.) (Kuno, 1966; Dickinson and Hatherton, 1967; Dickinson, 1968;

Nielson and Stoiber, 1973; Sugisaki 1976; Ui and Aramaki, 1978) and H_2O contents (Sakuyama, 1981). These parameters have been correlated with the depth of the Wadati-Benioff zone; crustal thickness, Bouguer gravity anomalies and the plate convergence rate.

One such example is shown in Figure 11 (Coulon and Thorpe, 1981). These correlations have been interpreted in terms of: (1) different depth of fractional crystallization, (2) different degree of partial melting, (3) different degree of contamination by crustal rocks during magma ascent.

In these mechanisms, important elements are the density contrast $\Delta\rho$ between the crust and the magma and the viscosity η in the upper mantle both of which control the depth of partial melting, fractionation and the residence time of the magma in the upper mantle and the crust.

Since M_w represents the strength of coupling, it may be proportional to the horizontal compressive stress $\Delta\sigma$ in the upper plate. Although $\Delta\sigma$ is of the order of 10 to 100 bars, it is comparable to the deviatoric stress responsible for ascent of mantle diapirs. Numerical models of diapirs show that $\Delta\sigma$ affects the velocity of magma ascent, and works in the same manner as $\Delta\rho$ and μ in controlling the composition of volcanic rocks at island arcs.

In order to explore this possibility, we examined the correlation between M_w and K_2O (at SiO_2 57 to 1 %) content, and M_w and the percentage of basalt for various island arcs. The results are shown in Figures 12 and 13. Despite fairly large scatter in the data, correlations seem to indicate that the regional variation of the horizonal compressive stress represented by M_w is at least partially

responsible for the regional variation of volcanic rocks.

In the course of this study, we found a rather serious difficulty in obtaining a uniform data set for volcanic rocks. This study is still at a preliminary stage, and we are collecting and compiling more data from various sources.

Flow and stress in subduction zone regions

Subduction zones provide excellent places for comparison of numerical models and observations. Seismicity in Benioff zones reveals the location of subducted slabs and reflects the state of stress within slabs.

Earthquakes in subduction zones are not uniformly distributed. The variation of earthquake activity with depth is presumably related to 1) variations of viscosity with depth, 2) variations of density with depth or 3) some time dependent process that involves plate ages, convergence rates, temperature and kinetics. The various parameters of each subduction zone, e.g., number of earthquakes, energy release, age of lithosphere, convergence rate, total length of subduction zone, dip, age of associated arc, presence of back-arc spreading, are being assembled.

The number of earthquakes and the energy release as a function of depth are particularly interesting. Most Benioff zones exhibit an exponential die off of activity from the surface to about 250 km. When old lithosphere, > 45 m.y., is subducted there is generally a secondary peak in activity between 300 and 670km. There are clearly at least two populations of events. In some cases there is a more gradual decay of activity in the upper mantle followed by an abrupt drop at 200-250 km

depth.

Graduate student Marius Vassiliou and Professor Anderson have classified different regions into three categories, depending upon their seismicity (see Table and Figure 14). In Class 1, seismicity ceases near 250km, with more or less linear decay to that depth. In Class 2, the deepest seismicity is near 550 km. This class is divided into two subclasses. In the first (2a), the decay is roughly linear above ~250 km below which there is a gap, and a separate peak centered around 4400-500 km. In the second (2b), the decay is also roughly linear above ~250 km. (although less so than in 2a), after which there is a break in slope, and a slower decay to ~550 km. Class 3, where the deepest seismicity is around 670 km, is likewise divided into two subclasses. In (3a), there is detached deep peak, with shallow seismicity extending to ~250 km. In (3b), there is continuous seismicity, with a break in the decay slope at ~250 km, a low level of seismicity below that, and a resurgence at 500-600 km. Regions in Class 1 tend to involve subduction of fairly young crust, and those in Classes 2 and 3 tend to involve subduction of older crust. Each class may represent a stage in the evolution of subduction. Plausible sequences of evolution might be 1 → 2a → 3a or 1 → 2b → 3b.

The seismicity presumably reflects stress in the slab. Vassiliou and Hager are computing finite element models of flow and stress near subducted slabs. An example of stress in a vertically sinking slab is shown in Figure 15. There is a roughly linear decrease in stress in the upper part of the slab, which could explain the seismicity observations nicely if the number of earthquakes depended exponentially on the stress

(e.g., Mogi, 1962). The increase in stress in the lower part of the slab is suggestive of Class 3 regions. Models are being extended to investigate the effect of slab dip and coupling the slab to the surface plate.

Professor Hager has investigated the deformation of the 670 km seismic discontinuity in these models. If convection is confined to the upper mantle by chemical stratification, slabs should penetrate 25-150 km into the lower mantle below the average depth of this discontinuity. Seismic data collected by Research Fellow Ichiro Nakanishi should help to resolve this important question.

The location of Benioff zone seismicity constrains the mantle flow pattern since it reveals the position of subducted slabs. Professor Hager extended his previous global flow models to include the effects of trench migration and increased strength of subducted slabs. He found that considering these effects does not alter his previous conclusion that for the Newtonian mantle viscosities derived from postglacial rebound studies, flow confined to the upper mantle does not match the observed dips of subducted slabs. Mantle-wide circulation passes this important test.

Seismic array studies

Studies done by graduate student Marianne Walck using the Caltech-U.S.G.S. SCARLET array are providing data which promise to provide useful constraints on our understanding of geodynamical processes. In a study with Bernard Minster, Walck studied lateral heterogeneities in P-wave velocities beneath Southern California. She was able to explain P-wave travel time anomalies in terms of a thin lens

model at a depth of 150 km. One possible interpretation of this anomaly is that it is due to alignment of olivine crystals in a downwelling flow beneath the Big Bend in the San Andreas fault. Hager is developing the mathematical formulation of a three-dimensional flow model to test this hypothesis.

Walck is now using the array in a study with Professor Anderson to study upper mantle structure beneath western Mexico and Gulf of California. The velocity gradient between the 400 km and 650 km discontinuities is well constrained and similar to that for northern Eurasia.

An important, unanswered question in Southern California geodynamics is the mechanism for the support of the Transverse Ranges, which reach elevations in excess of 10,000 ft. The extent to which these mountains are supported by crustal thickness variations is being explored by graduate student Thomas Hearn in conjunction with Minster. Hearn is using delay times of P_n arrivals, shown in Figure 16, to examine crustal thickness variations. The presence of a crustal root beneath the Sierra Nevada is confirmed. Thin crust, less than 20 km, occurs in the Salton Trough and extends into Arizona. Thickness of over 30 km are prevalent throughout the Transverse Ranges.

Table 1.
Distribution of Regions in the 3 Classes
(see text)

CLASS 1	CLASS 2		CLASS 3	
	Subclass 2a	Subclass 2b	Subclass 3a	Subclass 3b
N. Mexico	Japan	Izu-Bonin	Tonga	N. Chile
S. Mexico-C. Amer.	Kuriles	Solomon Islands		Peru
Ryukyus	Kermadec	Kamchatka		
Gr. Antilles	Marianas	Philippines		
L. Antilles	Banda	Java		
Greece				
S. Sandwich				
C. Chile				
Alaska				
Aleutians				
Sumatra				

Figure Captions

Figure 1: Records of long period surface waves excited by the eruption of Mt. St. Helens, May 18, 1980.

Figure 2: Amplitude spectra of Love (G) and Rayleigh (R) waves from the Mt. St. Helens eruption as a function of azimuth.

Figure 3: Radiation patterns for a single horizontal force, a single vertical force, and an isotropic source.

Figure 4: Synthetic seismograms for various source time histories compared with that observed for the Mt. St. Helens eruption.

Figure 5: Cartoon representing two of the three contributions to geoid anomalies in a fluid earth. A density contrast σ within the mantle induces flow. This flow results in stresses at the surface and core-mantle boundary, which deform. This deformation also causes a geoid anomaly. A third effect, added stresses resulting from the gravity field from σ acting on the mantle, is not shown.

Figure 6: Ratio of δV^{ℓ}_{TOT} to δV_{σ} as a function of depth to the density contrast and spherical harmonic degree for a uniform viscosity mantle. The total potential is of opposite sign than that for a rigid earth, δV_{σ}. For large ℓ the magnitude of the total geoid anomaly is much greater than that which would result in a rigid earth.

Figure 7: Flow vectors and streamlines for a passive ridge model with nonNewtonian (power law three) rheology. The various dashed lines depict the volume of the mantle sampled for a 6 km

thick basaltic crust generated by partially melting a given fraction of the mantle.

Figure 8: Migration of seismic activity after the New Hebrides earthquake of October 24, 1980 shown on a bathymetric map of the area. The heavy line outlines the zone of initial activity. An outward migration of activity is evident. The cluster of events in the fourth frame (10/26) are normal fault events seaward of the trench.

Figure 9: The correlation between earthquake size and: convergence rate and oceanic lithosphere age. The number at each subduction zone is the characteristic M_W (or M_S) value, and the regression plane is shown as contours of constant M_W. The broken line encloses the subduction zones (in the lower left corner) where there is either confirmed or suspected back-arc spreading. The important trend is that the largest earthquakes occur in subduction zones with a faster rate and younger age (see Ruff and Kanamori, 1980, for details).

Figure 10: The difference in the source time histories and inferred asperity distributions of the 1964 Alaskan and 1963 Kurile Islands earthquakes. The seismograms are shown at top as the solid traces. The dashed traces are the synthetic seismograms corresponding to the deconvolved source time functions shown beneath the seismograms. While the Kurile Islands time function is composed of a multiple event sequence, the Alaskan time function represents a smooth rupture spreading over a large area. Notice the large

difference in the seismic moments also. As discussed in Ruff and Kanamori (1981), the time functions of these events can be interepreted as the spatial distribution of asperities. The epicenters (stars) and fault areas are shown below, and the inferred asperities are indicated as the hachured areas. The Alaskan earthquake occurred in a region of huge asperity length scale.

Figure 11: Correlation between crustal thickness and crustal parameters (from Coulon and Thorpe, 1981).

Figure 12: Correlation between maximum earthquake size and potassium content.

Figure 13: Correlation between maximum earthquake size and basaltic component of volcanics.

Figure 14: Logarithm of number of earthquakes versus depth, with a depth interval of 20 km., for earthquakes occurring since 1964 with $m_b > 4$ for some regions to illutrate the different classes referred to in the text. (a) = Ryukyus, an example of Class 1. (b) = Japan, Class 2a. (c) = Java, Class 2b. (d) = Tonga, Class 3a. (e) = Peru, Class 3b.

Figure 15: Stress magnitude and velocity in slab for a finite element model of a vertical sinking slab.

Figure 16: Contours of delay times (in units of 0.1 sec) relative to station ABL. One second of relative delay time results from a relative thickness variation of 10 km, given uniform crustal velocity. Negative delay times indicate a thinner or slower crust.

Mt. St. Helens

MAJO $\Delta = 70.4^\circ$. $\phi = 303^\circ$

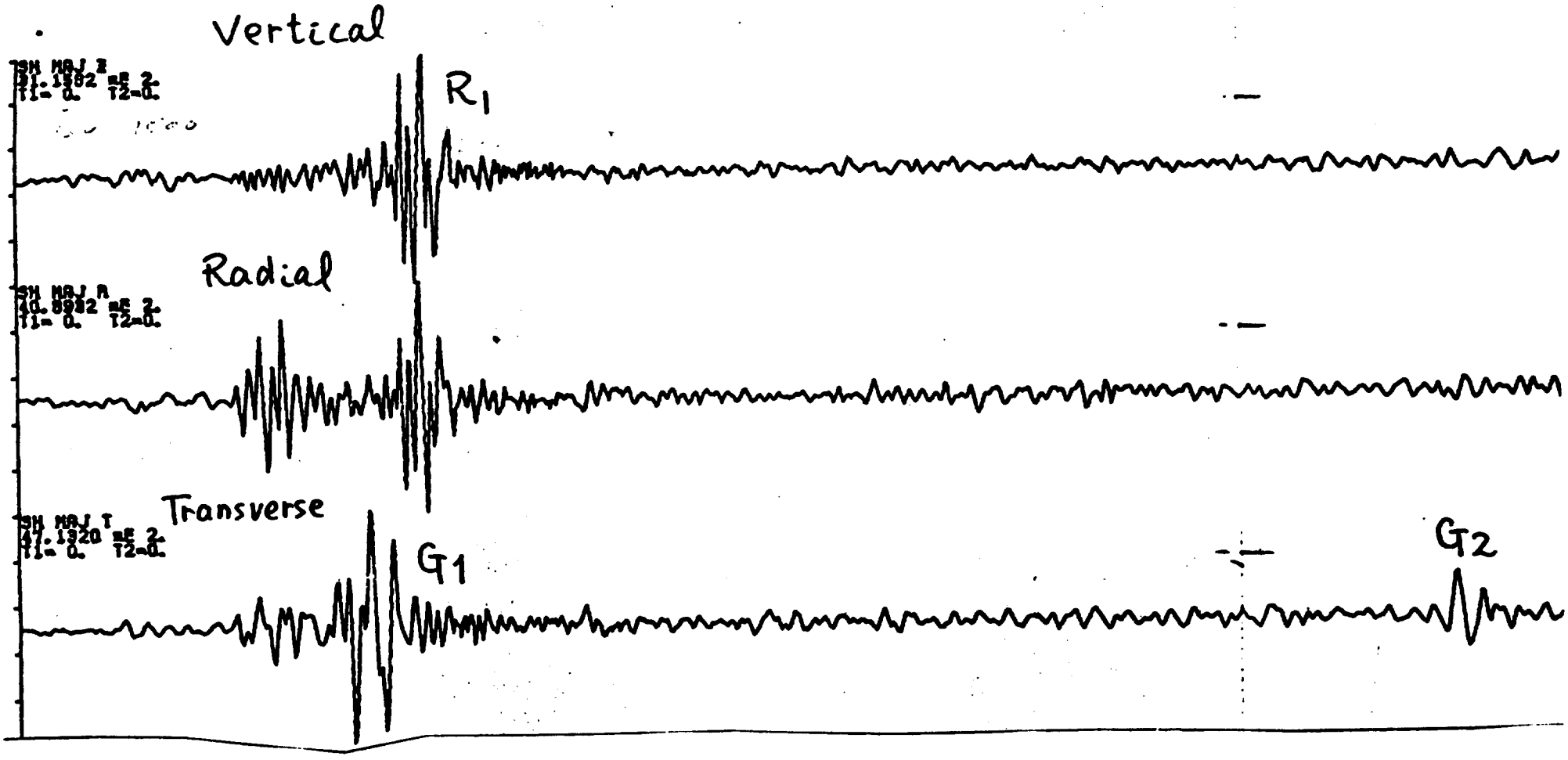

Fig. 1a

Mt. St. Helens

KONO $\Delta = 67.2°$ $\phi = 24.2°$

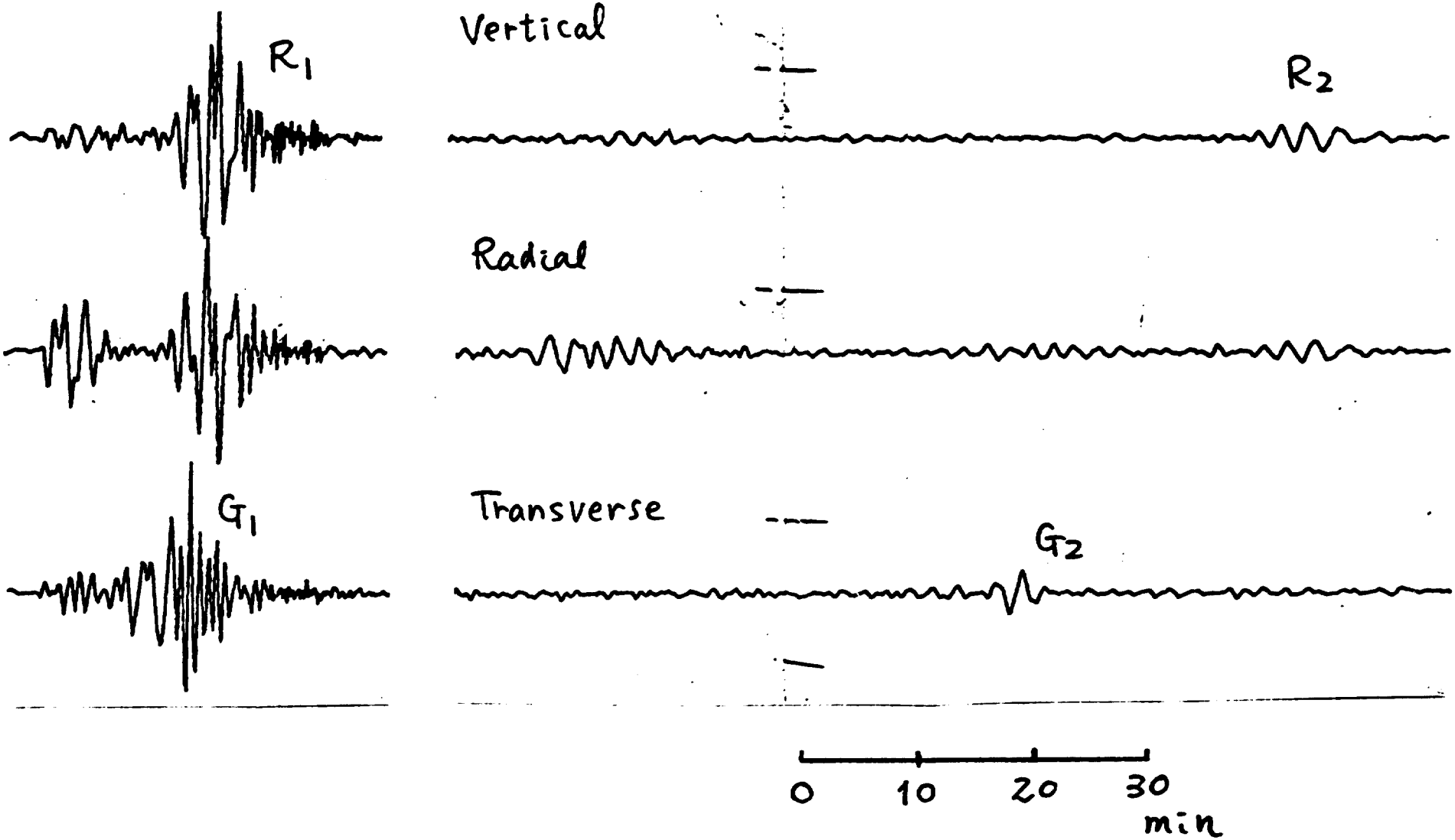

Fig. 16

Mt. St. Helens

NWAO $\Delta = 133.4°$, $\phi = 265°$

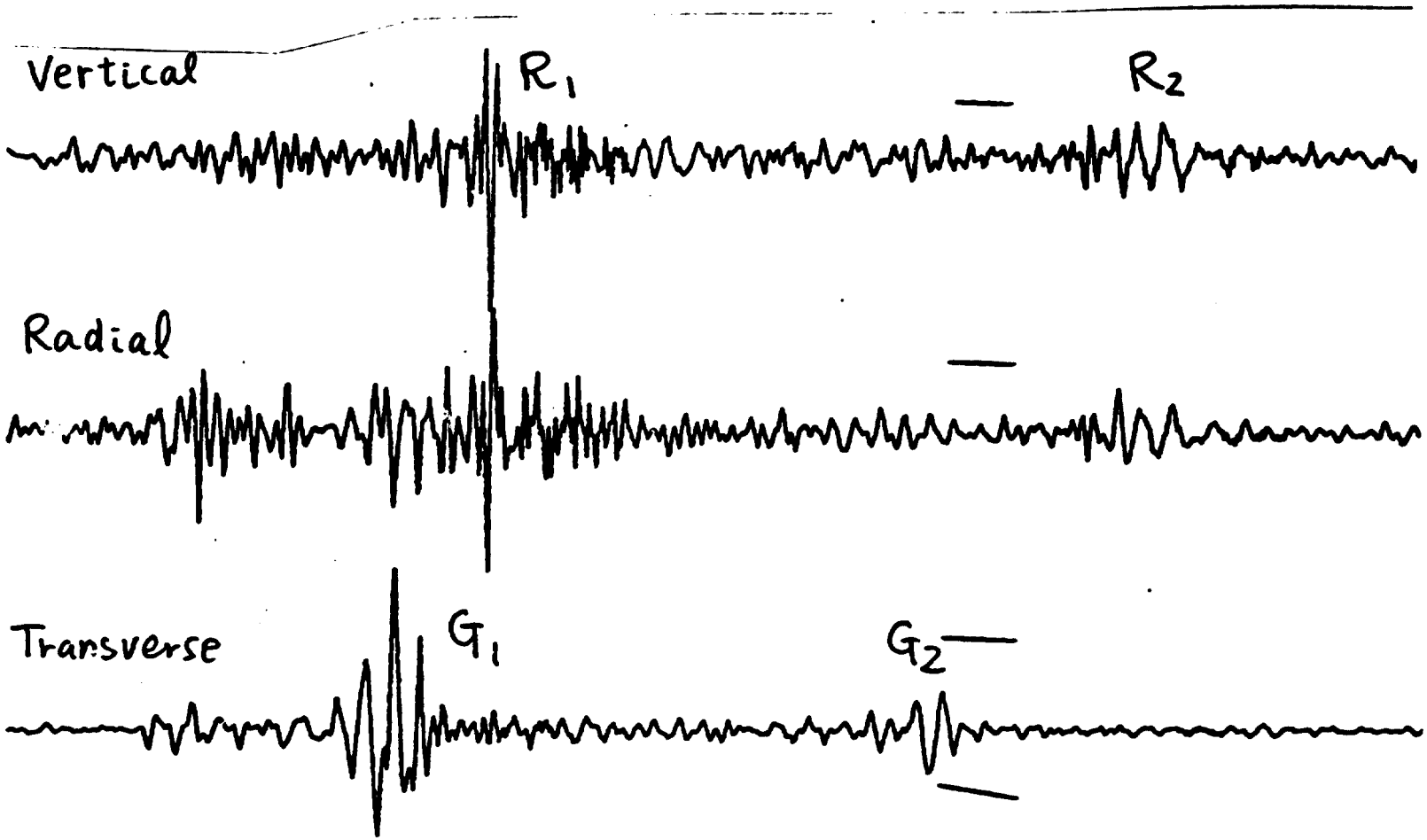

Fig. 1c

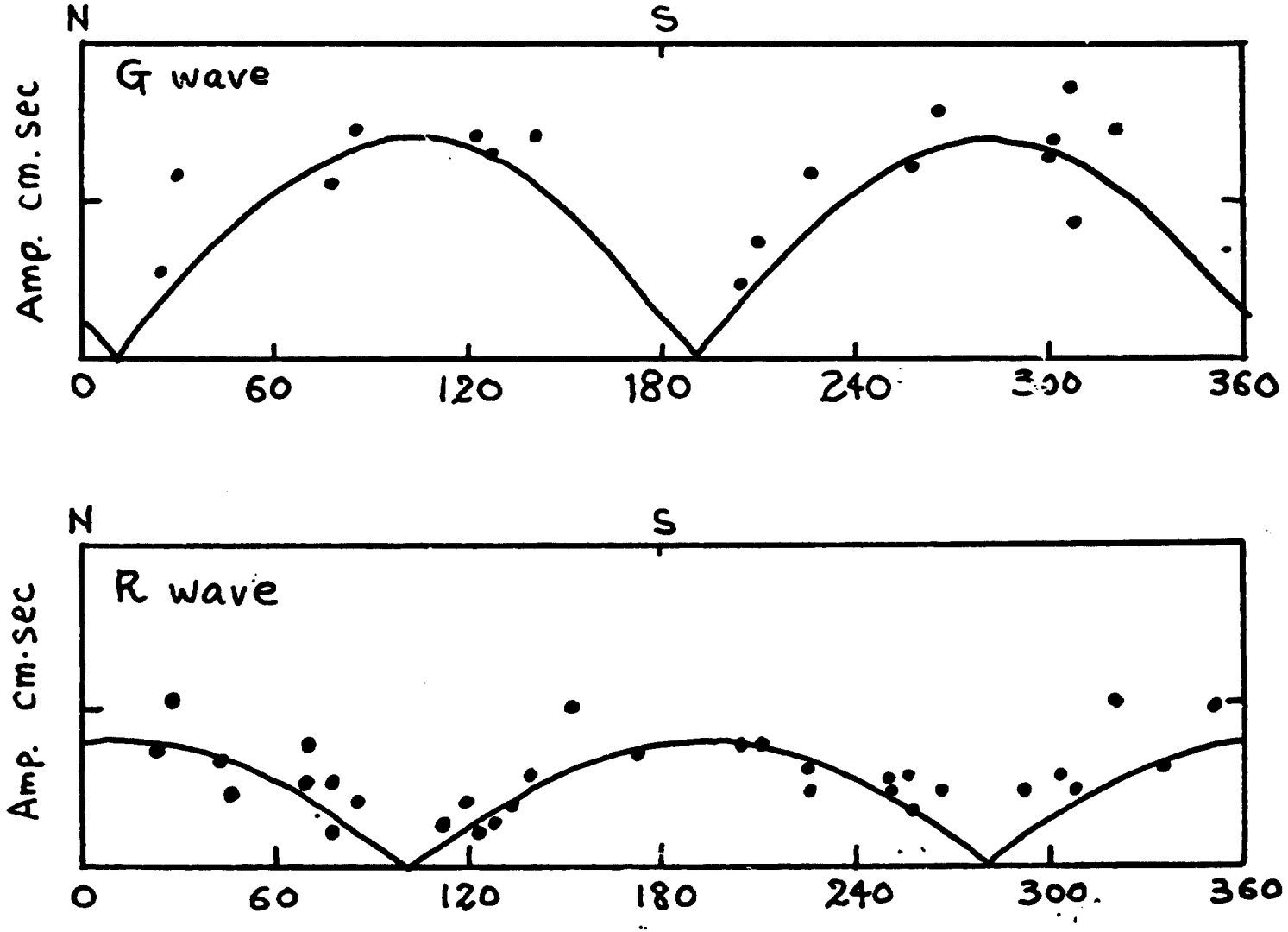
N
S
G wave
Amp. cm. sec
0
60
120
180
240
300
360
N
S
R wave
Amp. cm. sec
0
60
120
180
240
300
360

Fig. 2

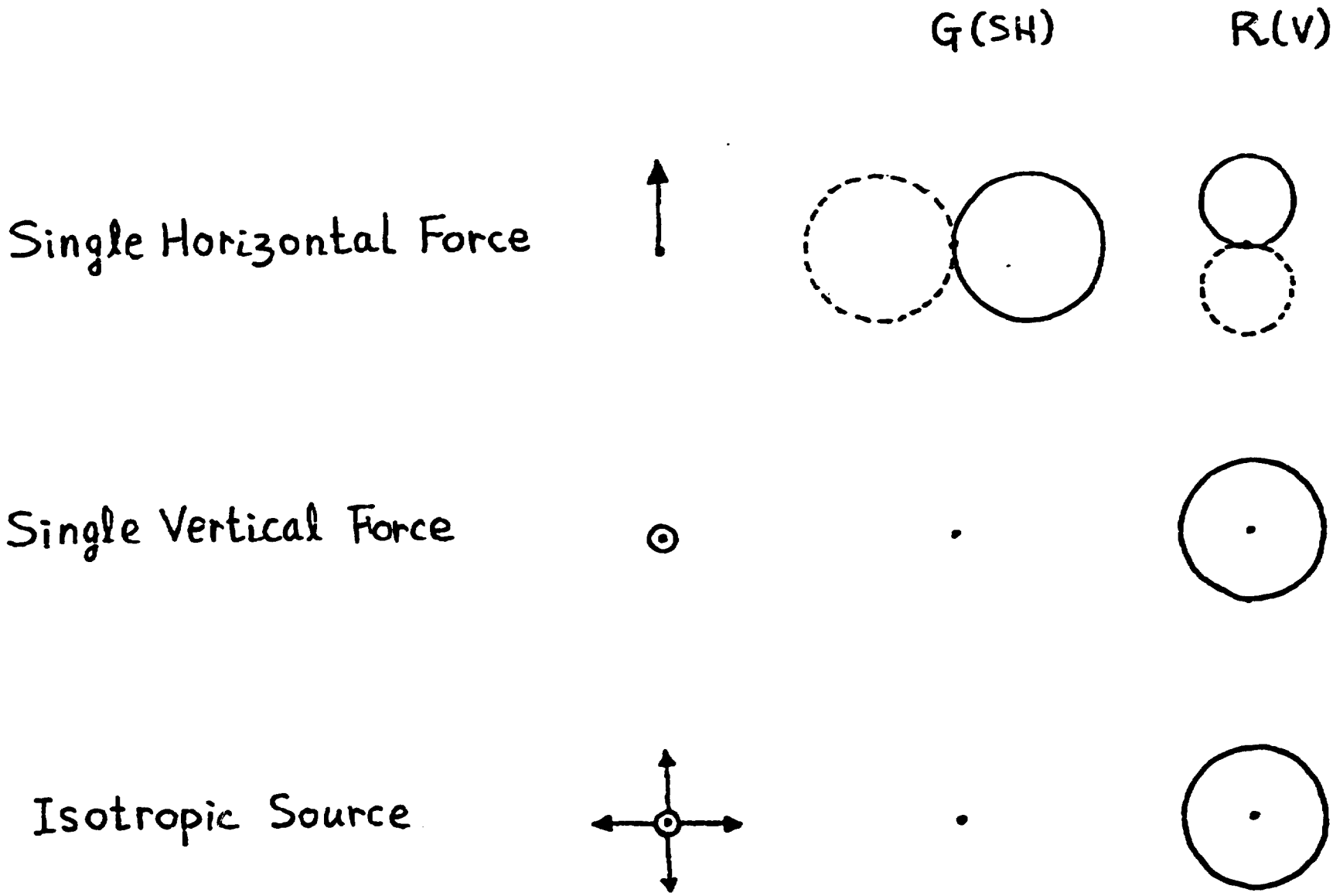
G(SH)
R(V)
Single Horizontal Force
Single Vertical Force
Isotropic Source

Fig. 3

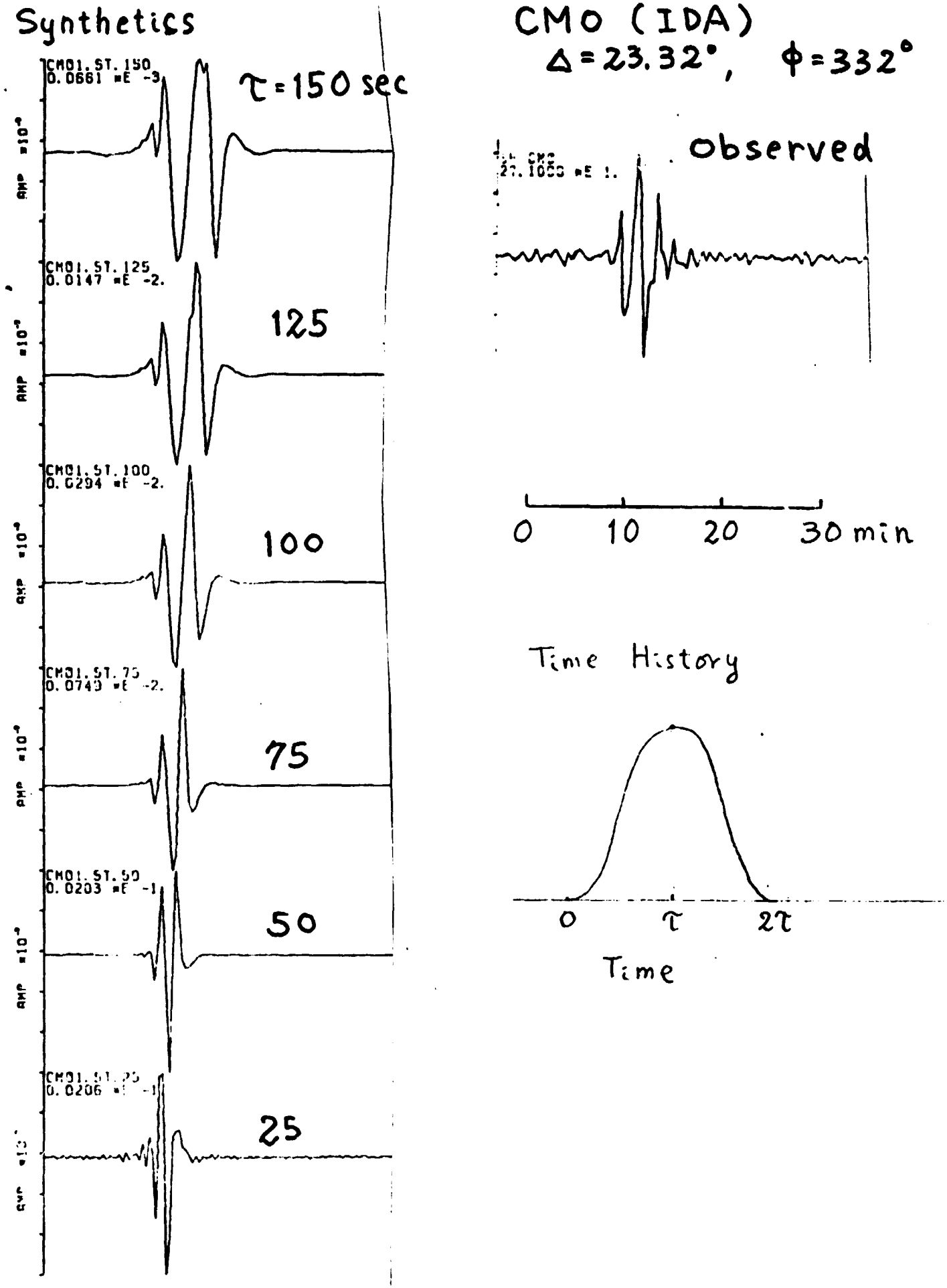
Synthetics
CMO (IDA)
Δ=23.32°, φ=332°
τ=150 sec
125
100
75
50
25
Observed
0 10 20 30 min
Time History
0 τ 2τ
Time

Fig. 4

Rigid Boundaries

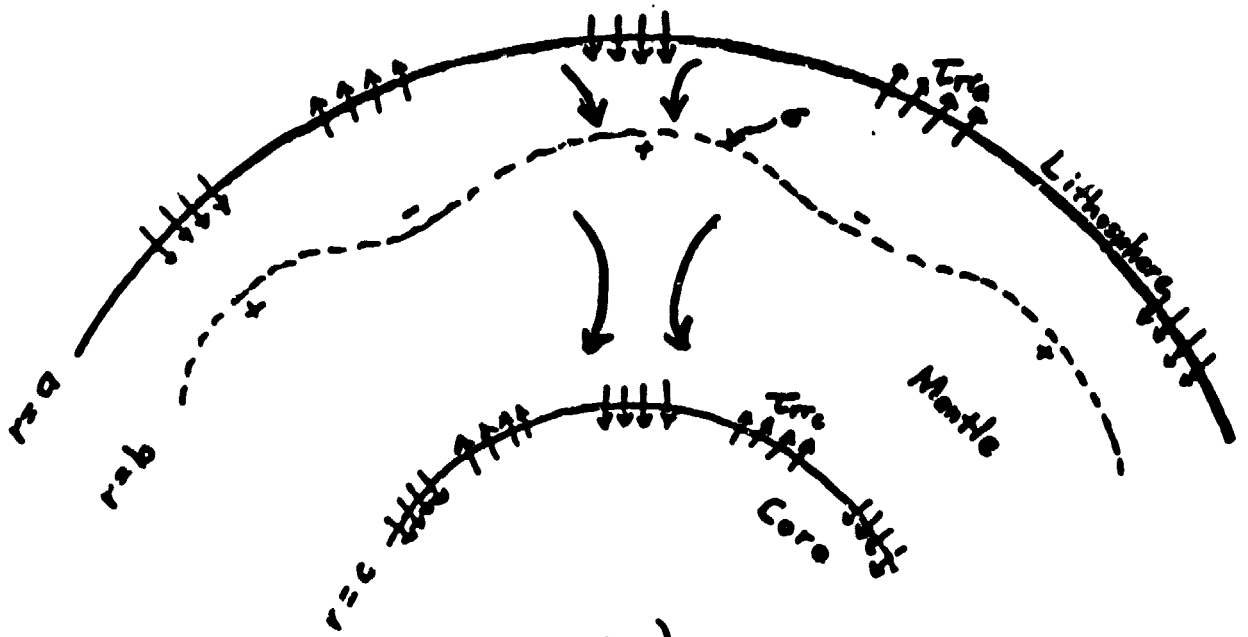

(a)

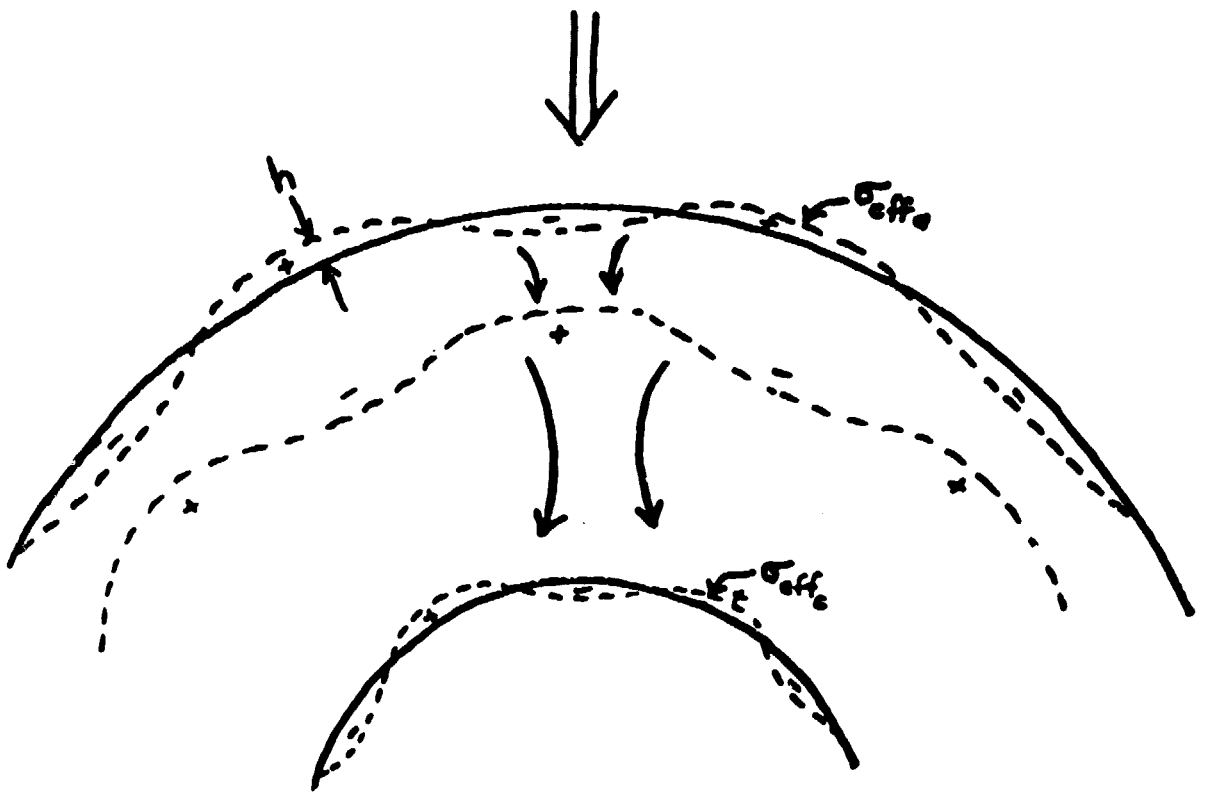

Relaxed Boundaries

(b)

Fig. 5

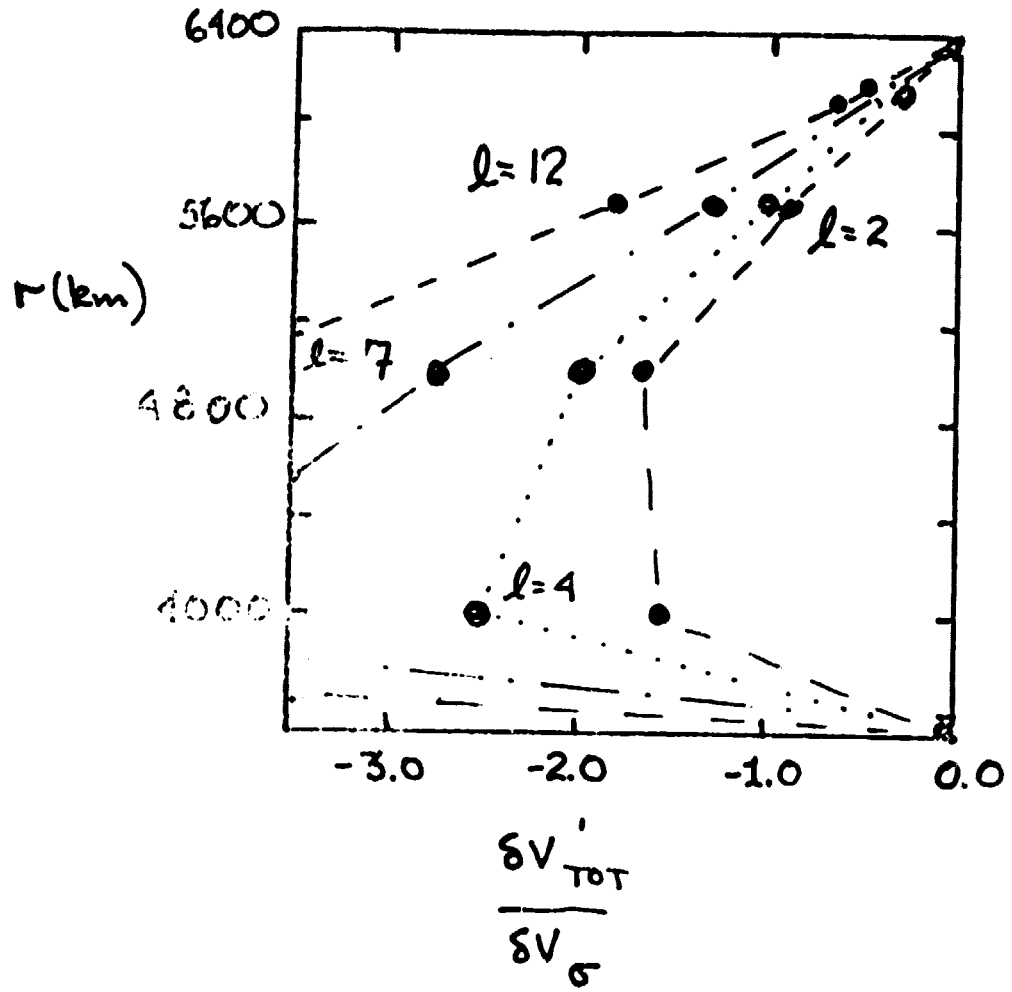

FIG 6

PASSIVE RIDGE

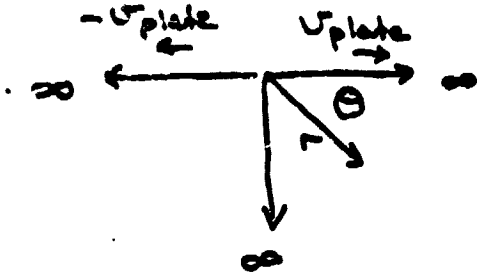

$\dot{\varepsilon} \propto \tau^3$ (power law creep)

$\mu_{eff} = \frac{\mu_0}{\tau^2}$

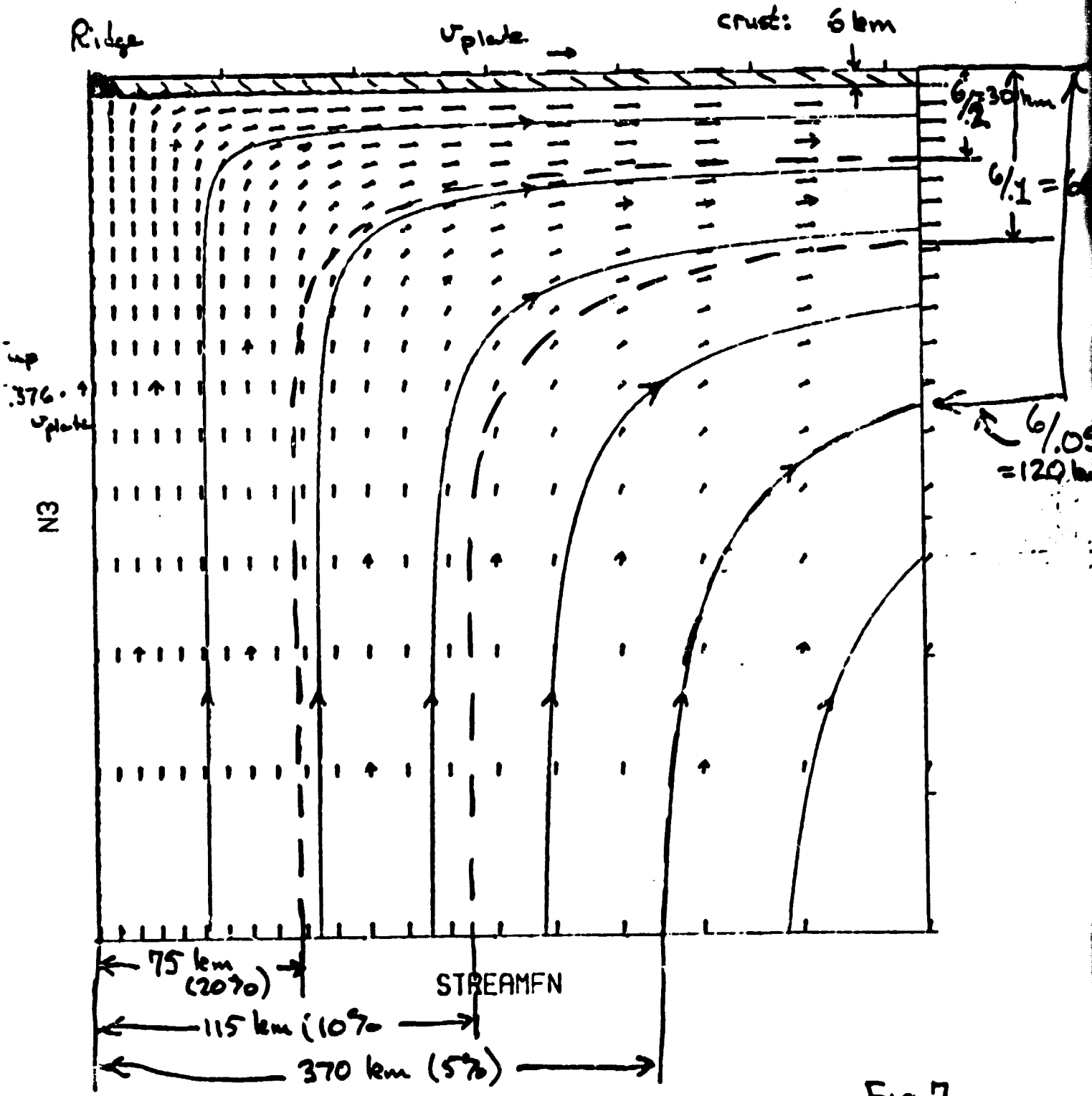

Fig 7

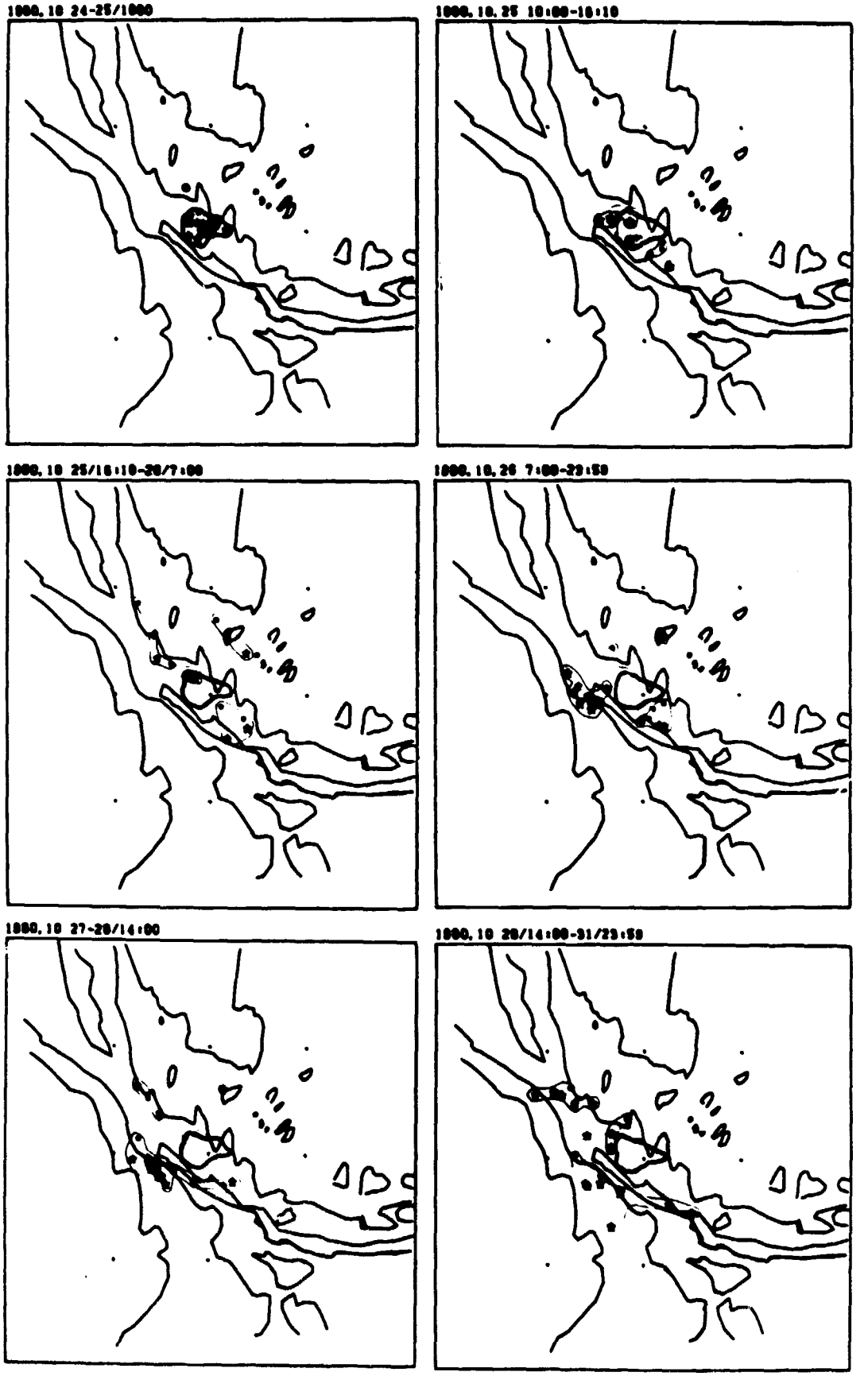
1990. 10 24-25/1000
1990. 10. 25 10:00-16:10
1990. 10 25/16:10-26/7:00
1990. 10. 26 7:00-22:50
1990. 10 27-28/14:00
1990. 10 28/14:00-31/23:59

Fig 8

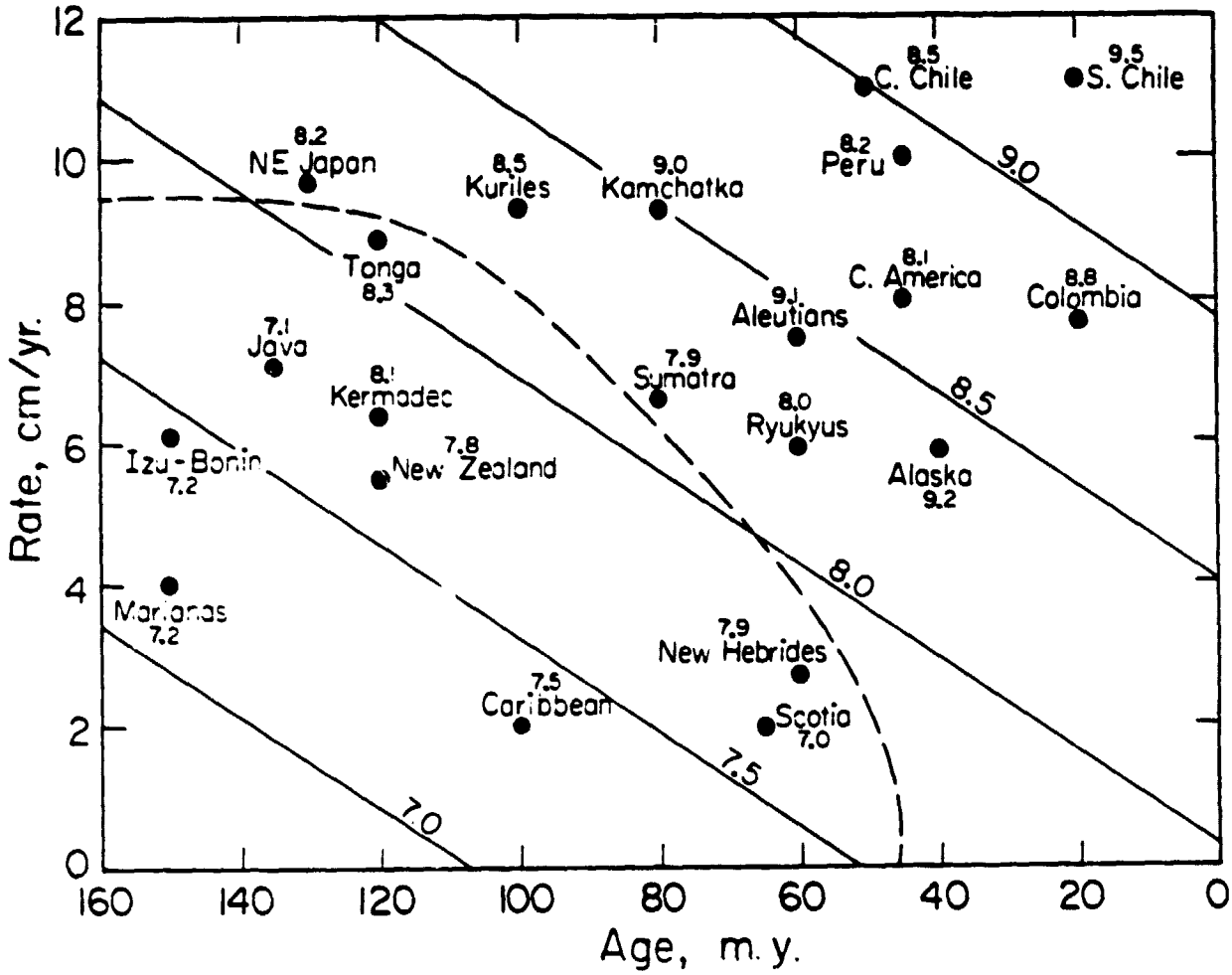
Rate, cm/yr.
Age, m.y.
0
2
4
6
8
10
12
160
140
120
100
80
60
40
20
0
8.5
C. Chile
9.5
S. Chile
8.2
NE Japan
8.5
Kuriles
9.0
Kamchatka
8.2
Peru
9.0
Tonga
8.3
8.1
C. America
8.8
Colombia
9.1
Aleutians
7.1
Java
7.9
Sumatra
8.5
8.1
Kermadec
8.0
Ryukyus
7.8
New Zealand
Izu-Bonin
7.2
Alaska
9.2
8.0
Marianas
7.2
7.9
New Hebrides
7.5
Caribbean
Scotia
7.0
7.5
7.0

Fig. 9

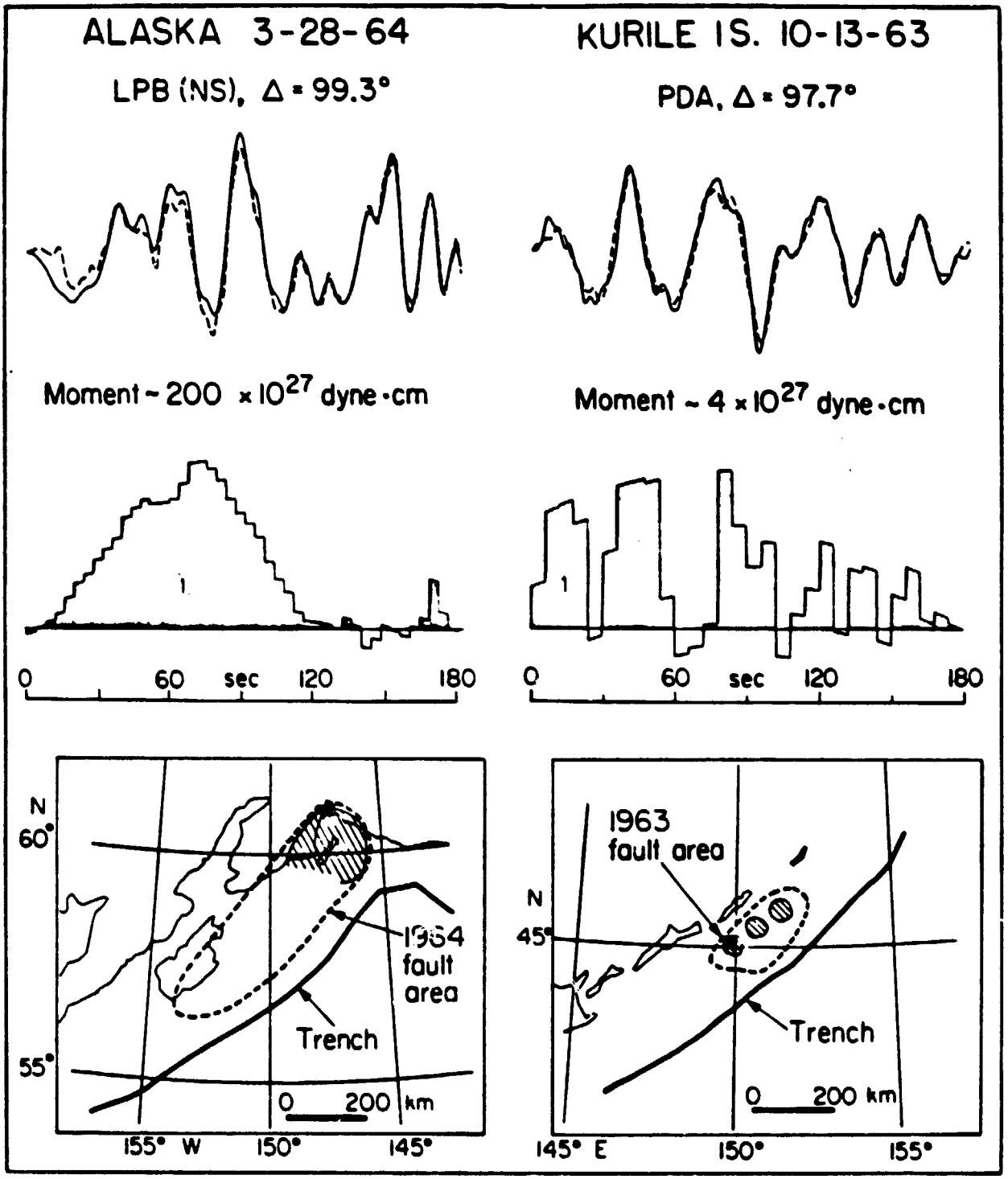
ALASKA 3-28-64
LPB (NS), Δ = 99.3°
KURILE IS. 10-13-63
PDA, Δ = 97.7°
Moment ~ 200 x 10^27 dyne·cm
Moment ~ 4 x 10^27 dyne·cm
1
1
0
60
sec
120
180
0
60
sec
120
180
N
60°
55°
1964
fault
area
Trench
0 200 km
155° W
150°
145°
1963
fault area
N
45°
Trench
0 200 km
145° E
150°
155°

Fig. 10

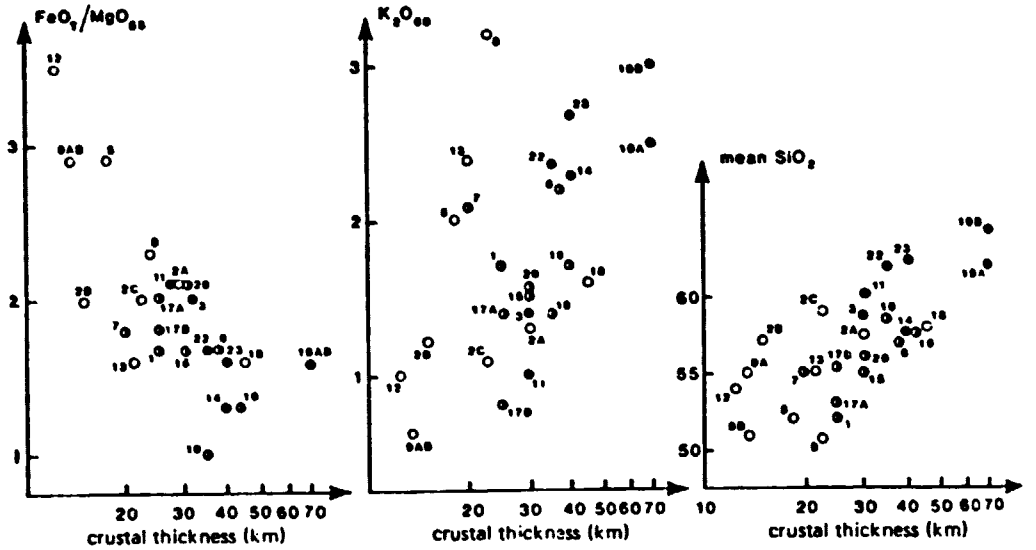
FeO_t/MgO_{ss}
3
2
1
20 30 40 50 60 70
crustal thickness (km)
K_2O_{ss}
3
2
1
20 30 40 50 60 70
crustal thickness (km)
mean SiO_2
60
55
50
10 20 30 40 50 60 70
crustal thickness (km)

Fig. 11

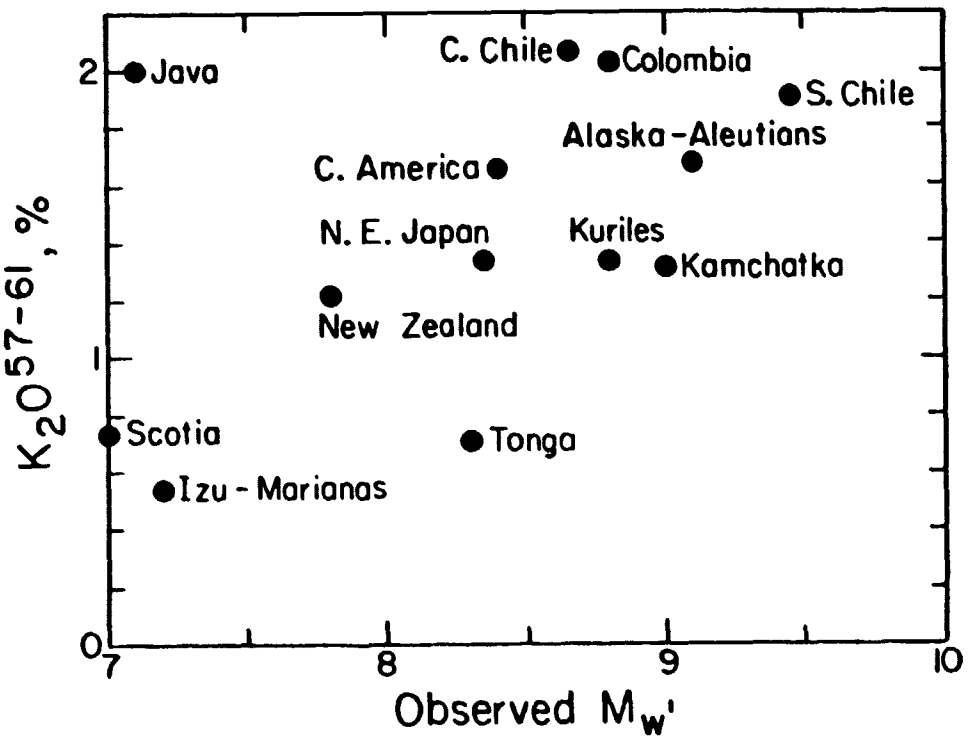
C. Chile
Colombia
Java
S. Chile
Alaska-Aleutians
C. America
N. E. Japan
Kuriles
Kamchatka
New Zealand
Scotia
Tonga
Izu-Marianas
2
1
0
7
8
9
10
K_2O^{57-61}, %
Observed $M_{W'}$

Fig. 12

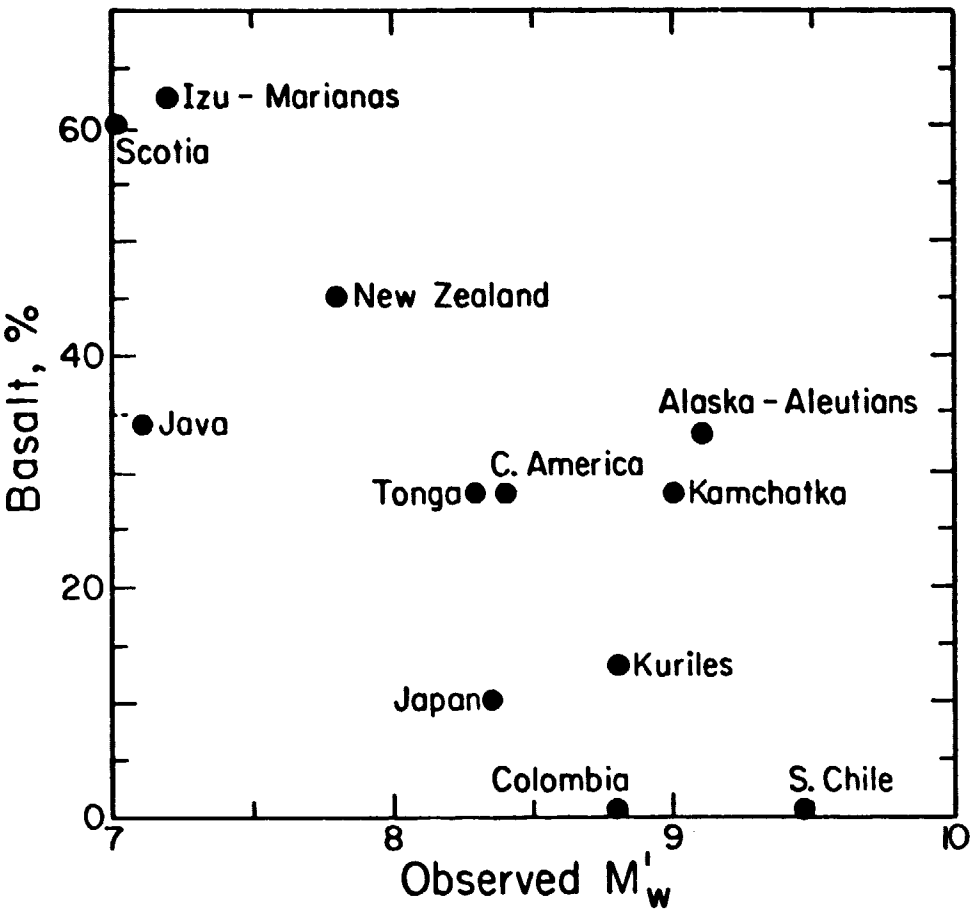
Izu - Marianas
Scotia
New Zealand
Java
Alaska - Aleutians
C. America
Tonga
Kamchatka
Kuriles
Japan
Colombia
S. Chile
Basalt, %
0
20
40
60
7
8
9
10
Observed M'_w

Fig. 13

Fig 19

FIG. 15

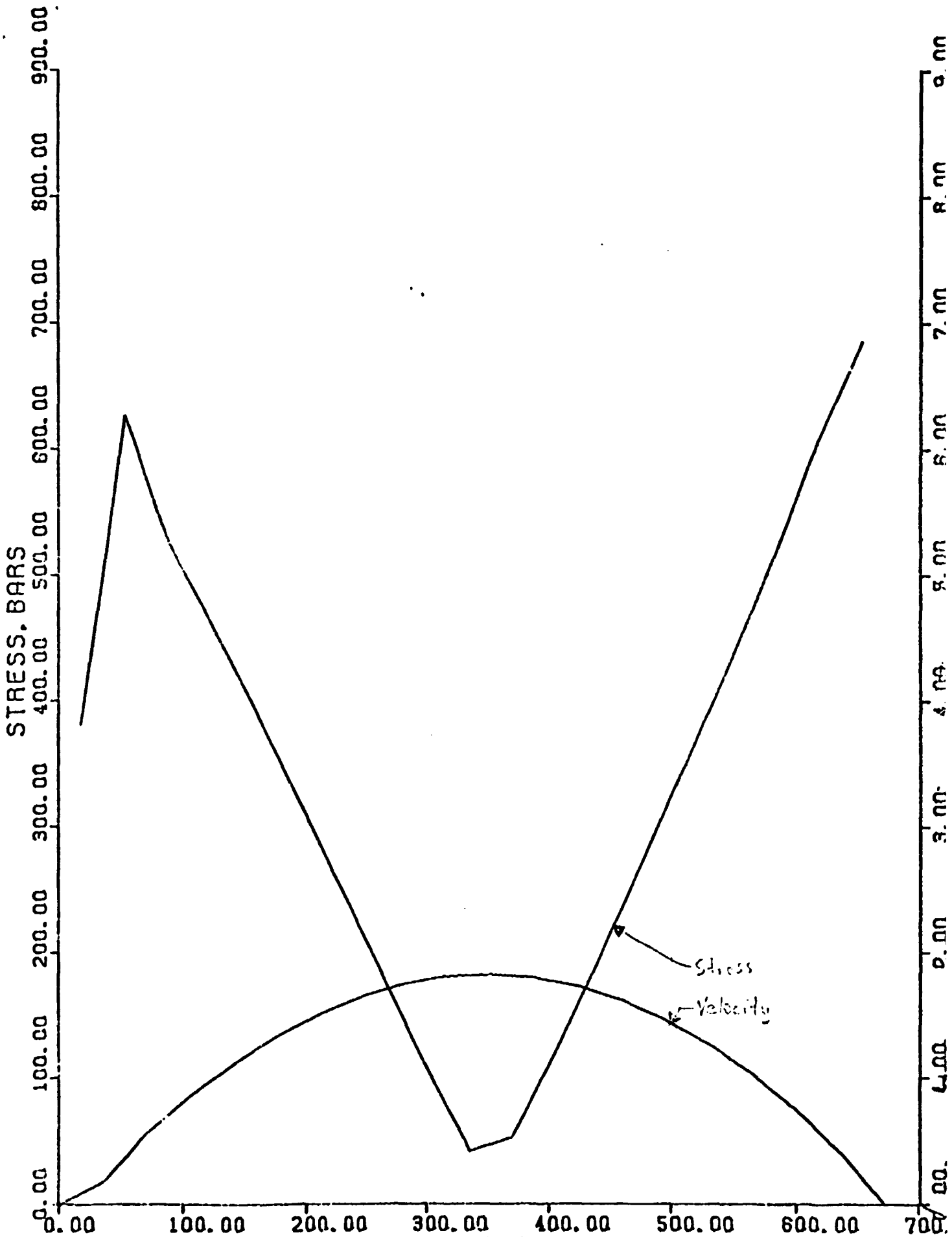
STRESS, BARS
0.00
100.00
200.00
300.00
400.00
500.00
600.00
700.00
800.00
900.00
0.00
100.00
200.00
300.00
400.00
500.00
600.00
700.00
800.00
900.00
Stress
Velocity

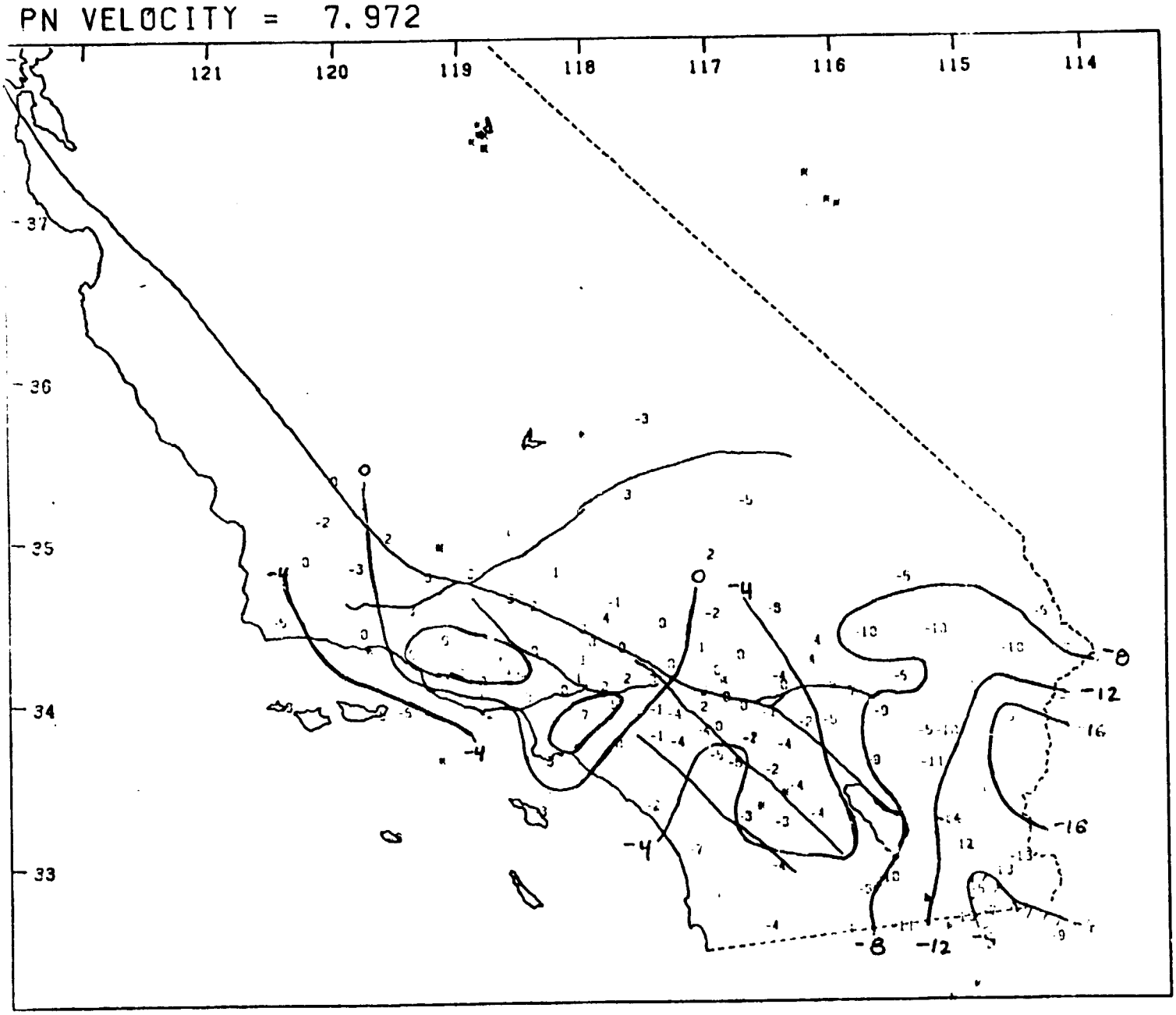

Fig 16

PAPERS IN PRESS

AND

ABSTRACTS

Submitted to:

Geodynamic Series of the
American Geophysical Union

A GLOBAL GEOCHEMICAL MODEL FOR THE EVOLUTION OF THE MANTLE

Don L. Anderson

Seismological Laboratory, California Institute of Technology

Pasadena, California 91125

Abstract. Basalt, eclogite, and harzburgite, differentiation products of the Earth, appear to be trapped in the upper mantle above the 670 km seismic discontinuity. It is proposed that the upper mantle transition region, 220 to 670 km, is composed of eclogite, or olivine eclogite, which has been derived from primitive mantle by about 20% partial melting and that this is the source and sink of oceanic lithosphere. The remainder of the upper mantle is garnet peridotite, or pyrolite, the source of continental basalts and hotspot magmas. This region is enriched in incompatible elements by partial melts or hydrous and CO_2 rich metasomatic fluids which have depleted the underlying layers in the L.I.L. elements and L.R.E.E. The eclogite layer is internally heated. It may control the convection pattern in the upper mantle. Material can only escape from this layer by melting. The insulating effect of thick continental lithosphere may lead to partial melting in both the peridotite and eclogite layers. Hotspots and ridges would then mark the former locations of continents. Most of the basaltic or pyroxenitic fraction of the oceanic lithosphere returns to the eclogite layer.

In this model plate tectonics is intermittent. At a depth of 150-220 km the continental thermal anomaly triggers kimberlite and carbonatite activity, alkali and flood basalt volcanism, vertical tectonics and continental breakup. Hotspots remain active after the continents leave, building the oceanic islands. Mantle plumes rise from a depth of about 220 km. Midocean ridge basalts originate in the depleted layer below this depth. Material from this layer may also be displaced by subducted oceanic lithosphere to form back-arc basin magmas.

Introduction

Although convection plays an important role in plate tectonics and heat transport in the Earth, it has not succeeded in homogenizing the mantle. Magmas are still being produced from mantle reservoirs which have remained separate for the

Submitted to:

Geophyscial Research Letters

PLATE TECTONICS ON VENUS

Don L. Anderson

Seismological Laboratory, California Institute of Technology

Pasadena, California 91125

Abstract. The high surface temperature of Venus implies a permanently buoyant lithosphere and a thick basaltic crust. Terrestrial style tectonics with deep subduction and crustal recycling is not possible. Overthickened basaltic crust partially melts instead of converting to eclogite. Because mantle magmas do not have convenient access to the surface the ^{40}Ar abundance in the atmosphere should be low. Venus may provide an analog to Archean tectonics on the Earth.

Introduction

The surface of Venus is about 450 K warmer than the surface of the Earth. This affects the buoyancy, thermal expansion, thermal conducticity and, hence, the thermal evolution and ultimate fate of the lithosphere. The pressure in the upper mantle of Venus is at least 12% less than at equivalent depths in the Earth's upper mantle. Thus, the depth of melting, the locations of upper mantle phase changes and the viscosity of the upper mantle will be different for the two planets. The buoyancy and thermal properties of the lithosphere control the style of plate tectonics and the associated time and length scales. Most discussions of the comparative tectonics between Earth and Venus address only the differences in viscosity.

The oceanic lithosphere of the Earth cools as it ages and it eventually becomes denser than the underlying mantle. This instability develops after about 40 m.y. (Oxburgh and Parmentier, 1977). Once cooling reaches a depth of 50 km the garnet pyroxenite or eclogite transformations may make a substantial contribution to the negative buoyancy of the lithosphere. Continents and oceanic plateaus resist subduction because of their thick low-density crusts. The fate of the terrestrial lithosphere, therefore, depends on both chemistry and temperature. The purpose of this paper is to investigate the implications for Venus tectonics of its high surface temperature. We will conclude that the surface

Upper Mantle Anisotropy; Evidence from Free Oscillations

Don L. Anderson[1]
and
Adam M. Dziewonski[2]

[1]Seismological Laboratory
California Institute of Technology
Pasadena, California 91125

[2] Department of Geological Sciences
Harvard University
Cambridge, Massachusetts 02138

Short title: Upper mantle anisotropy

February 11, 1981
Revised May 15, 1981
Revised May 19, 1981

Submitted to: Geophys. J. R. Astrom. Soc.

Summary

Isotropic Earth models are unable to provide uniform fits to the gross Earth normal mode dataset or, in many cases, to regional Love and Rayleigh wave data. Anisotropic inversion provides a good fit to the data and indicates that the upper 200 km of the mantle is anisotropic. The nature and magnitude of the required anisotropy, moreover, is similar to that found in body wave studies and in studies of ultramafic samples from the upper mantle. Pronounced upper mantle low-velocity zones are characteristic of models resulting from isotropic inversion of global or regional datasets. Anisotropic models have more nearly constant velocities in the upper mantle.

Normal mode partial derivatives are calculated for a transversely isotropic Earth model with a radial axis of symmetry. For this type of anisotropy there are five elastic constants. The two shear type moduli can be determined from the toroidal modes. Spheroidal and Rayleigh modes are sensitive to all five elastic constants but are mainly controlled by the two compressional-type moduli, one of the shear-type moduli and the remaining, mixed-mode, modulus. The lack of sensitivity of Rayleigh waves to compressional wave velocities is a characteristic only of the isotropic case. The partial derivitives of the horizontal and vertical components of the compressional velocity are nearly equal and opposite in the region of the mantle where the shear velocity sensitivity is the greatest. The net compressional wave partial derivative, at depth, is therefore very small for isotropic perturbation. Compressional wave anisotropy, however, has a significant effect on Rayleigh wave dispersion. Once it has been established that

transverse anisotropy is important it is necessary to invert for all five elastic constants. If the azimuthal effect has not been averaged out a more general anisotropy may have to be allowed for.

Introduction

There is a growing body of evidence that much of the upper mantle may be anisotropic to the propagation of seismic waves. The early evidence was the discrepancy between Rayleigh wave and Love wave dispersion (Anderson, 1961, 1966, Anderson and Harkrider, 1962) and the azimuthal dependence of oceanic P_n velocities (Raitt et al., 1971, Hess, 1964). Azimuthal variations have now been documented for many areas of the world (Bibee and Shor, 1976, Bamford, 1977) and the Rayleigh-Love discrepancy is also widespread (McEvilly, 1964, Aki, 1968, Forsyth, 1975, Yu and Mitchell, 1979, Schlue and Knopoff, 1977). Shear wave birefringence, a manifestation of anisotropy, has also been reported (Anderson, 1966, Hirn, 1977, Masataka et al., 1980). The degree of anisotropy varies but is typically about 5%. It is not known to what depth the anisotropy extends but some of the data requires it to depths as great as 200 km.

Anderson (1966) proposed that the "discrepancy" between mantle Rayleigh and Love waves could be explained if the vertical P and S velocities in the upper mantle were 7-8% less than the horizontal velocities. He also showed that models without an upper mantle low-velocity zone, such as the Jeffreys model, could satisfy the dispersion data if the upper mantle was anisotropic. The Love-Rayleigh discrepancy has survived to the present and models have been proposed which have SV in the upper mantle less than SH by about 4%. These more

Absorption Band Q Model for the Earth

Don L. Anderson and Jeffrey W. Given

Seismological Laboratory
California Institute of Technology
Pasadena, California 91125

August 20, 1981
August 21, 1981

In Preparation

BROADWAY TYPESETTING 1-12 bjw 4168
Caltech Galley 1

Submitted to:

Special Issue of the
Journal of Geophysical Research

THE PHYSICS OF CREEP AND ATTENUATION IN THE MANTLE

Don L. Anderson and J. Bernard Minster

Seismological Laboratory, California Institute of Technology, Pasadena, California 91125

Abstract. Dislocations contribute to both seismic wave attenuation and steady-state creep in the mantle. The two phenomena involve quite different strains and characteristic times but they can both be understood with simple dislocation models. The most satisfactory model for creep involves the glide of dislocations across subgrains and rate limited by the climb of jogged dislocations in the walls of a polygonized network. The jog formation energy contributes to the apparent activation energy for creep, making it substantially larger than the activation energy for self-diffusion. The theory leads to either a σ^2 or σ^3 law for creep rate, depending on the length of the dislocations relative to the equilibrium spacing of thermal jogs.

Attenuation in the mantle at seismic frequencies is probably caused by the glide of dislocations in the subgrains. Kink and impurity drag can both contribute to the glide time constant. The kink-formation, or Peierls barrier, model for dislocation glide appears to be a low-temperature, high-frequency mechanism most appropriate for pure systems. A small amount of impurity drag brings the dislocation glide characteristic time into the seismic band at upper-mantle temperatures.

The attenuation and creep behavior of the mantle are related through the dislocation structure. Discussion of the various possible mechanisms is facilitated by casting them and the geophysical data in terms of a pre-exponential characteristic time and an activation energy. The relaxation strength is an additional parameter that can be used to identify the attenuation mechanism. Mobile dislocations in subgrains, rather than cell walls, have the appropriate characteristics to explain the damping of seismic waves in the upper mantle. The grain boundary peak may be responsible for attenuation in the lithosphere.

I. Introduction

The purpose of this paper is to investigate the role of dislocations in both creep and attenuation. The high temperature creep of most crystalline solids is controlled by dislocation climb or glide plus climb [Weertmann, 1968]. For a wide variety of metallic, ionic, and polar crystals the activation energies for creep and self-diffusion are esentially identical, indicating that the motions of dislocations are rate-limited by self-diffusion. Furthermore, in the stress range of about 10^{-2} to 10^{-5} G, where G is the shear modulus, the stress exponent of the creep rate is about 3, which is consistent with dislocation climb or the glide of jogged dislocations. Both of these mechanisms of steady-state creep require self-

GLOBAL MANTLE FLOW AND COMPARATIVE SUBDUCTOLOGY

Bradford H. Hager
Seismological Laboratory
California Institute of Technology
Pasadena, CA 91125

Richard J. O'Connell
Department of Geological Sciences
Harvard University
Cambridge, MA 02138

Arthur Raefsky
Jet Propulsion Laboratory and Seismological Laboratory
California Institute of Technology
Pasadena, CA 91125

July 31, 1981

Submitted to:

Tectonophysics - Special Issue, Symposium
on Convergence and Subdivision

Texas A & M university

April, 1981

Abstract

Subducted slabs penetrate a convecting, actively flowing mantle. Some of the variations observed among subduction zones may result from differences in the global flow pattern and thereby provide constraints on mantle flow models. We compute global flow models by solving for flow in a viscous sphere subject to the observed plate velocities as boundary conditions. Density contrasts assumed appropriate for the surface plates and subducted slabs are included. Models are considered in which flow extends throughout the mantle or in which flow is confined to the upper mantle.

For both types of model, all subduction zones which are currently undergoing back-arc spreading are characterized by a shear in the asthenosphere tending to pull the overriding plate toward the trench. All island arcs which are not undergoing back-arc spreading, with the possible exception of Sunda, have the opposite sense of shear contributing to back-arc compression. Instantaneous flow velocity vectors match observed Benioff zone dips for the model which allows mantle wide flow, but not for the upper mantle model considered, which has a viscosity of 10^{22}p. The maximum earthquake magnitude M_w observed for island arcs is well correlated with age of the subducted slab and pressure gradient between the trench and back-arc region if flow extends throughout the mantle. The effect on particle trajectories of trench migration is not important if subducted slabs sink faster than trenches migrate. Variation in slab dip and seismic coupling can be explained by global flow if flow extends throughout the mantle. If flow is confined to the upper mantle, its effective viscosity must be substantially less than 10^{22}p.

REASSESSMENT OF A REPORTED S-DELAY UNDER TRINDADE

H. C. Nataf, T. Lay, D. L. Anderson

Seismological Laboratory, California Institute of Technology, Pasadena, CA 91125

and E. A. Okal

Dept. of Geology & Geophysics, Yale University, P.O. Box 6666, New Haven, CT 06511

Submitted to:

Geophysical Research Letters

Abstact. We present a correction to a paper by Okal and Anderson (1975) about multiple ScS travel-time anomalies. We have reanalyzed data for ScS_2 surface bounces in the South Atlantic Ocean. From these data an ScS_2-S residual of 23.6 seconds was found by Okal and Anderson (1975). This corresponded to an ScS_2 surface bounce point under Trindade island and was inferred to be due to very slow upper mantle associated with the Trindade hot spot. The analysis we present here invalidates this conclusion. The nature of the upper mantle under Trindade is an open issue.

Introduction

It is possible to use ScS_2-ScS time anomalies to estimate S travel-time heterogeneities in the upper mantle below the surface bounce point of ScS_2. The time difference between ScS_2 and ScS or S is obtained by cross-correlation of the two signals. The residual is the difference from the predicted time using Jeffreys-Bullen (JB) tables (1958). This method was used by Okal and Anderson (1975) -hereafter referred to as O&A- with data from the WWSS long period network. O&A obtained travel time residuals for bounces under continents and oceans. Among their numerous data, one is of special interest both because it gives the largest delay and because it corresponds to the unique case of a surface bounce under a 'hot spot'. Indeed O&A found an 11.8 seconds one-way travel-time residual corresponding to an ScS_2 surface bounce point under Trindade island in the South Atlantic Ocean (see figure 1). Trindade's volcanism is as young as 1 million years ,and extremely silica undersaturated,suggesting origin from a hydrous mantle (Oversby,1971;Valencio and Mendia,1974). This led O&A to propose that the large S delays which they observed were due to reflection in a very slow upper mantle, possibly indicating a higher degree of partial melting under the hot spot. In this paper we present a detailed analysis of the data O&A used to reach this conclusion. We show that for the South Atlantic data points O&A used the SV component instead of the SH component. In fact,the stations used are on a node of the SH radiation pattern. Besides the fact that waveform distortion might occur on the SV component,we show that in this particular case the first arrival corresponds to the interference of three phases; SKS,S and ScS. Moreover we examine seismograms for stations

SEISMIC COUPLING AND UNCOUPLING AT SUBDUCTION ZONES

Larry Ruff and Hiroo Kanamori

Seismological Laboratory
California Institute of Technology
Pasadena, CA 91125

July 16,1981, Revised August 2,1981

Submitted to: Tectonophysics special issue,
Symposium on Convergence and Subduction,
Texas A&M University, April, 1981.

Abstract

Seismic coupling has been used as a qualitative measure of the "interaction" between the two plates at subduction zones. Kanamori (1971) introduced seismic coupling after noting that the characteristic size of earthquakes varies systematically for the northern Pacific subduction zones. A quantitative global comparison of many subduction zones reveals a strong correlation of earthquake size with two other variables: age of the subducting lithosphere and convergence rate. The largest earthquakes occur in zones with young lithosphere and fast convergence rates, while zones with old lithosphere and slow rates are relatively aseismic. Results from a study of the rupture process of three great earthquakes indicate that maximum earthquake size is directly related to the asperity distribution on the fault plane (asperities are strong regions that resist the motion between the two plates). The zones with the largest earthquakes have very large asperities, while the zones with smaller earthquakes have small scattered asperities. This observation can be translated into a simple model of seismic coupling, where the horizontal compressive stress between the two plates is proportional to the ratio of the summed asperity area to the total area of the contact surface. While the variation in asperity size is used to establish a connection between earthquake size and tectonic stress, it also implies that plate age and rate affect the asperity distribution. Plate age and rate can control asperity distribution directly by use of the horizontal compressive stress associated with the "preferred trajectory" (i.e. the vertical and horizontal velocities of subducting slabs are determined by the

plate age and convergence velocity). Indirect influences are many, including: oceanic plate topography and the amount of subducted sediments.

All of the subduction zones are apparently uncoupled below a depth of 40 km, and we propose that the basalt to eclogite phase change in the down-going oceanic crust may be largely responsible. This phase change should start at a depth of 30-35 km, and could at least partially uncouple the plates by superplastic deformation throughout the oceanic crust during the phase change.

RELATIVE ARRAY ANALYSIS OF UPPER MANTLE LATERAL VELOCITY VARIATIONS IN SOUTHERN CALIFORNIA

Marianne C. Walck

J. Bernard Minster*

Seismological Laboratory, California Institute of Technology

Pasadena, California 91125

July 2, 1981

Submitted to:

Journal of Geophysical Research

*present address: Systems, Science and Software, Inc., P.O. Box 1620,

La Jolla, California 92038

ABSTRACT

Spatial averaging of short-period teleseismic P-wave arrivals across SCARLET constrains upper mantle lateral velocity variations beneath southern California. We compare $dT/d\Delta$, back-azimuth and averaged arrival time estimates determined from the entire network for 154 events to the same parameters derived from small subsets of SCARLET. The resulting relative array diagrams and plots of "net subarray delays" computed for 171 overlapping subarrays exhibit large anomalies that vary smoothly as a function of subarray position, implying substantial lateral heterogeneity under the network. Patterns of mislocation vectors for more than 100 subarrays permits identification of an East-West striking high-velocity antiform beneath the Transverse Ranges. Further constraints on both the lateral configuration and depth of the anomaly are obtained through thin lens analysis of the net delay data. The best-fit lens -- at 150 km depth -- features low velocities beneath the Salton Trough as well as a concentrated high-velocity zone between 116.3° - 118.3°W and 33.7° - 34.8°N, consistent with the relative array diagrams and the PKP-delay contours of Hadley and Kanamori (1977). Therefore the bulk of the high-velocity material observed by Hadley and Kanamori may in fact lie at 150 km rather than 40 - 100 km. This possibility prompts renewed speculation regarding the relationship of this body to the plate tectonic history of the region.

MODELS OF FLOW AND STRESS BENEATH RIDGES

B. H. Hager (Seismo Lab, Caltech,
Pasadena, California 91125)

Two classes of models of flow beneath ridges are presented. Kinematic (passive) models of flow driven by the motion of the plates are calculated analytically for both Newtonian and power law rheologies. Plots of the deviatoric stress tensor are shown. For both rheologies the deviatoric stress below the ridge is zero, leading to the conclusion that shear heating from kinematic flow beneath ridges is of negligible importance in the generation of partial melts. Vertical flow for n=3 creep takes the form of a broad plug with the maximum upwelling velocity a factor of two smaller than that for Newtonian creep. Power law creep leads to a shallower sampling of the mantle beneath ridges, tending to isolate the deeper mantle.

In the second type model, we investigate the buoyant upwelling of a partially molten diapir. A model with Newtonian rheology is used as a basis of comparison for a series of models which employ more realistic rheologies. The effects on rheology of stresses generated by expansion due to increased melting are included.

1. AGU Chapman Conference on Generation of the Oceanic Lithosphere
2. Oral

DEFORMATION OF SEISMIC DISCONTINUITIES AND THE SCALE OF MANTLE CONVECTION

Bradford H. Hager
Arthur Raefsky (Both at: Seismological Laboratory, Caltech, Pasadena, CA 91125)

The stresses from the horizontal density contrasts in a convecting system cause deformation of the system boundaries. Readily observable examples of this effect are the ~4 km elevation of the seafloor at midoceanic ridges and the ~6 km depression at trenches. Numerical models show that for convection confined to the upper mantle almost the entire weight of the subducted lithosphere is compensated by deformation of the surface and 670 km discontinuity.

For a given stress, the deformation of an interface is inversely proportional to the density contrast across it. If the 670 km discontinuity were a chemical discontinuity, not a phase boundary, the deformation for a given stress would be 5-10 times that for the same stress at the surface. The distribution of this deformation depends upon the rheology of the lithosphere and mantle. Slab strength and decoupling by the asthenosphere cause stresses at 670 km to be much larger than those supported by deformation of the upper surface. Depression of the 670 km discontinuity beneath slabs would be at least 25 km and would likely reach 150 km. A flat discontinuity is compatible with a phase change with negligible Clapeyron slope but not with a chemical discontinuity; in particular, cessation of seismicity at the global average depth of the 670 km discontinuity is not compatible with a layered mantle.

Phase changes, coupled with deformation of chemical discontinuities, can lead to finite amplitude instabilities in mantle convection which result in episodic overturns on a large and small scale. This provides a mechanism for mixing between layers. Examples include extensive melting caused by pulling a chemical layer above its solidus and massive overturn of a layered mantle if a subducted slab penetrates deeply enough to undergo a phase change.

1. 1981 Fall Meeting

2. HAGE038920

3. Corresponding address:

Bradford H. Hager
California Institute of Technology, 252-21
Pasadena, CA 91125
213-356-6938

4. VGP

5. Special Session: (Chemical and Convective Stratification of the Mantle

6. O (oral)

7. 0%

8. a. Bill to:
Seismological Lab 252-21
Calif. Inst. of Tech.
Pasadena, CA 91125

b. P.O. 66-550500

c. Student rate not applicable

9. C (Contributed)

MODELS OF FLOW AND STRESS NEAR SUBDUCTED SLABS

B. H. Hager (Seismological Laboratory, 252-21, California Institute of Technology, Pasadena, California 91125)
A. Raefsky (Jet Propulsion Laboratory, Pasadena, California 91109)
R. J. O'Connell (Dept. of Geological Sciences, Harvard University, Cambridge, Massachusetts 02138)

One important observation constraining the dynamics of subduction is that plates are bent well beyond their elastic limits upon subduction, yet are then restraightened, rather than remaining curled. Another fundamental observation is that slabs do not in general have dips close to vertical. These observations imply that the net effect of tractions acting on the slab from viscous flow within the mantle is comparable to or larger than the negative buoyancy of the slab and much larger than the slab's resistance to bending. The angle of subduction, as well as the state of stress within the slab, is strongly influenced by the mantle flow. Observations of slab dip and state of stress, in combination with models of mantle flow, can help to constrain mantle rheology and provide a better understanding of the dynamics of plate motion and subduction.

Flow in the mantle is influenced by both the large-scale global flow associated with plate motions and small-scale flow driven by local density variations. Previously calculated kinematic models of the global flow driven by the (imposed) motion of the surface plates show that for models which allow return flow deep in the mantle, the instantaneous flow vectors match the observed dips of deep Benioff zones (Hager and O'Connell, Tectonophysics, 19 8). These models are highly simplified, however, in particular, neglecting the increased density of the slabs, the supposed increased strength of slabs relative to the asthenosphere, and the temporal evolution of plate boundaries.

New global models have been calculated which include the density contrasts appropriate to the subducted slabs, located on the basis of observed seismicity. For models which allow flow deep in the mantle, the match between instantaneous velocity vectors and Benioff zone dips is improved; velocities beneath subduction zones are close to the velocities of the surface plates, so presumably flow vectors closely match slab trajectories in magnitudes as well as dips. For the model in which flow is confined to the upper mantle, the constraints of return flow dominate and there is little change in velocity from the previous kinematic models. Flow cuts across the deep Benioff zones in the Sunda, Tonga, and Middle America regions.

Consideration of reasonable trench migration velocities has little effect on the models which allow deep mantle flow, although the shallow flow models are changed substantially. Although it is conceivably possible to manipulate shallow-flow models to match the observed dips of Benioff zones, the fact that the simple deep flow models match the dips so well is evidence that the flow associated with plate motions extends deep into the mantle.

Symposium on Convergence and Subduction
Texas A & M University
April, 1981

The effects of the likely relatively higher strength of the slab are investigated using a series of two-dimensional finite element models. Plausible contrasts in the effective viscosity of the slab relative to the asthenosphere have surprisingly little effect on the orientation of the flow lines. The local state of stress is more sensitive than velocities to variation in the rheology of the earth's interior.

Deviations from the Ruff and Kanamori (PEPI, 1980) empirical relation between seismic coupling, convergence velocity, and plate age appear to be related to regions where the global return flow is complicated; seismic zones where coupling is anomalously weak tend to be regions where the global flow exerts pressure on the upper surface of subducted slabs. Deep mantle flow may effect seismic coupling at shallow depths as well as slab dip and stress.

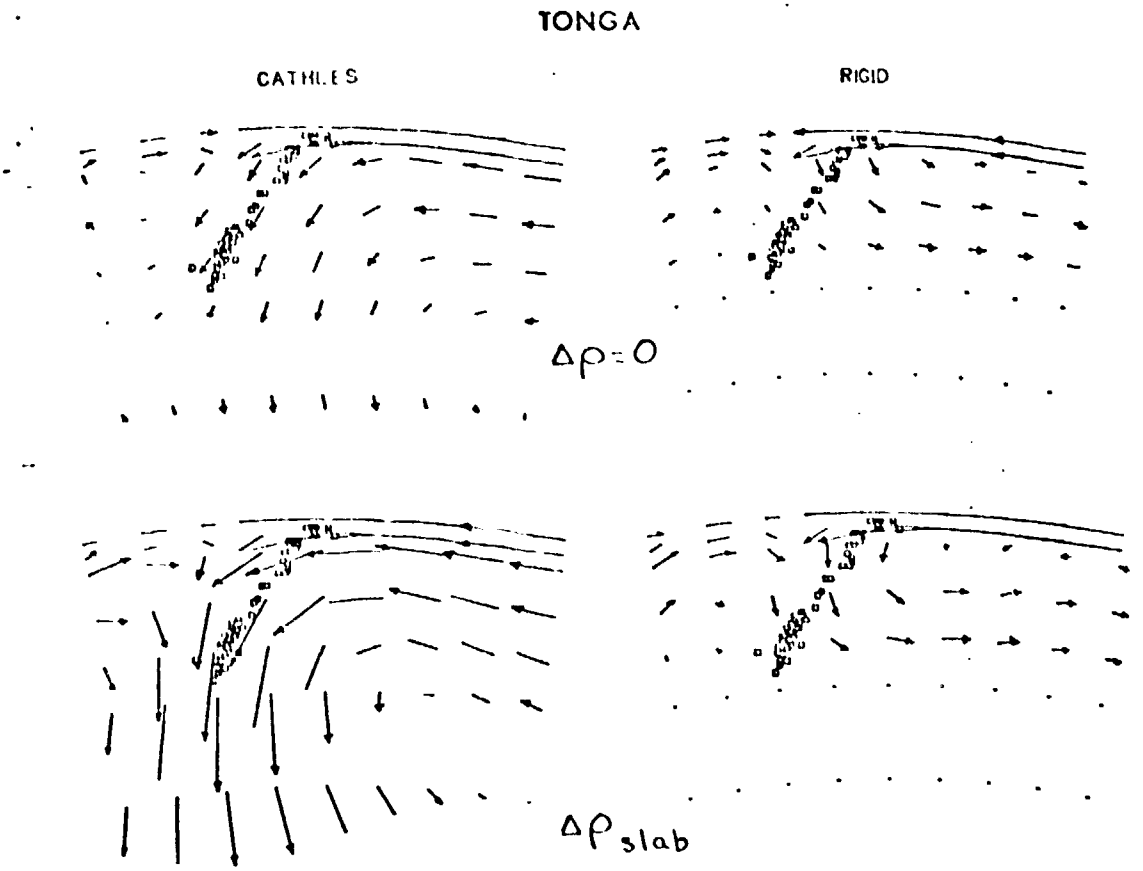

Sections through flow models in the Tonga region. The models on the left have a 10^{22} p lower mantle, while the models on the right have an effectively rigid lower mantle. In all the models, the observed plate velocities are imposed as boundary conditions. The lower row of models has a density contrast appropriate to a subducted slab in the region of earthquake hypocenters (marked by boxes). The displacements plotted represent the instantaneous place velocities extrapolated for 7 My.

TIME-TERM MAPPING OF THE MOHO DISCONTINUITY IN SOUTHERN CALIFORNIA

Thomas M. Hearn (Seismological Laboratory, California Institute of Technology, Pasadena, California 91125)
J. Bernard Minster (Systems, Science and Software, P.O. 1620, La Jolla, CA 92038)

The time-term method for the analysis of refraction data (Willmore and Bancroft, 1960) has been applied to Pn arrivals at the southern California seismic array. A combination of more than 30 earthquakes and 175 stations produce the data set of over 2000 Pn arrivals. The inversion finds a mean Pn velocity of 8.0 km/sec for the entire data set, however variations of .2 km/sec from this value are known to exist in southern California. The delay times computed are equivalent to the function $\int_0^h((1-V(z)^2/V_n^2)^{1/2}/V(z))dz$ where V(z) is the crustal velocity, V_n is the Pn velocity, h is the Moho depth and z is depth. The variation of over 1.5 seconds in the delay times is indicative of about 15 km of relief in the crust-mantle boundary.

A thinning of the crust to less than 20 km occurs in the Salton Trough with the thin crust apparently extending into southwest Arizona. A previous refraction study in Arizona (Warren, 1969) indicates a crustal thickness of 20 km southwest of Gila Bend. This suggests that the crustal thinning associated with the Gulf of California begins in the southeast California - southwest Arizona region. Crustal thickness in the Channel Islands averages about 24 km while thicknesses of over 30 km are prevalent throughout the Transverse Ranges. This is consistent with the higher Bouguer gravity anomalies of the Channel Islands. The high delay times of the Los Angeles and Ventura areas are due to the thick sedimentary sequences of the associated basins. The presence of a crustal root beneath the Sierra Nevada is confirmed by events at Mammoth which demonstrate a delay of more than .5 seconds for paths travelling directly along the batholith.

1. 1981 Fall Meeting
2. HEARN
3. Corresponding address:

   Thomas M. Hearn
   Caltech 252-21
   Pasadena, CA 91125
   213-356-6974
4. S (Seismology)
5. none
6. O (oral)
7. none
8. a. Bill to:
      Seismological Lab 252-21
      Calif. Inst. of Tech.
      Pasadena, CA 91125

   b. P.O. 66-550482

   c. Student rate applicable
9. C (Contributed)

MECHANISM OF MT. ST. HELENS ERUPTION DETERMINED FROM LONG-PERIOD SURFACE WAVES

Hiroo Kanamori
Jeffrey W. Given (both at: Seismological Laboratory, California Institute of Technology, Pasadena, California 91125)

The eruption of Mt. St. Helens on May 18, 1980 excited long-period (100 to 260 sec) surface waves, and high quality seismograms were recorded at many IDA, SRO and ASRO stations. These are probably the first data of this kind obtained for a volcanic event, and provide a unique opportunity to study the mechanism of eruption. The amplitude radiation patterns of both Rayleigh and Love waves are two lobed with a nodal direction in E 10° S for Rayleigh waves and in N 10° E for Love waves. This radiation pattern precludes any double couple mechanism. The radiation pattern, the initial phase, the relatively large amplitude ratio of Love to Rayleigh waves and the existence of clear nodes of the Rayleigh-wave radiation pattern suggest that the source is represented by an almost horizontal (less than 15° from the horizontal) single force pointed toward S 10° W; no isotropic component is allowed. The surface-wave spectra fall off very rapidly at periods shorter than 80 sec suggesting a very slow source process. Although the details of the source time history could not be determined, a smooth bell-shaped time function having a total duration of about 160 sec is considered appropriate on the basis of comparison of synthetic and the observed seismograms. The peak value of the force is about 10^{18} dynes. The result can be interpreted in terms of a northward lateral blast, a northward landslide or combination of both. The magnitude and the time history of the force provide important constraints on the physical mechanism of the eruption.

1. 1981 Fall Meeting

2. KANA 003573

3. Corresponding address:

   Seismological Laboratory
   California Institute of Technology
   Pasadena, California 91125

4. S (Seismology)

5. none

6. O (oral)

7. 0%

8. Bill to:

   Seismological Laboratory
   California Institute of Technology
   Pasadena, California 91125

   P.O.#66-550478

   Student rate not applicable

9. C

Seismicity and Volcanic Rock Series in Island Arcs

Hiroo Kanamori and Marius S. Vassiliou
Seismological Laboratory
California Institute of Technology
Pasadena, California 91125

Plate subduction is generally considered to be the ultimate cause of large earthquakes and volcanism at island arcs. The activity of large earthquakes can be related to various parameters of plate subduction. For example, the magnitude, M_w, of the largest characteristic earthquake for each subduction zone can be expressed reasonably well by a linear function of plate convergence rate and the age of the subducting slab (Ruff and Kanamori, 1980). On the other hand, various parameters for arc volcanic rocks have been associated with other characteristic features of island arcs. Among them are the ratio CA/TH (Calc-Alkali Series/Tholeiitic Series) (Miyashiro, 1974), Silica Index 0 (Sugimura, 1968), Alkali (K_2O, Na_2O etc.) (Kuno, 1966; Dickinson and Hatherton, 1967; Dickinson, 1968; Nielson and Stoiber, 1973; Sugisaki 1976; Ui and Aramaki, 1978) and H_2O contents (Sakuyama, 1981). These parameters have been correlated with the depth of the Wadati-Benioff zone; crustal thickness, Bouguer gravity anomalies and the plate convergence rate. We investigated various relations between seismic activity measured by M_w and the parameters for volcanic rocks to clarify the relation between the stress state at subduction zones and magma genesis discussed by Uyeda and Kanamori (1979). We found that CA/TH ratio and the alkali content correlate better with M_w than with the crustal thickness. Since a large value of M_w can be considered to be a result of increased tectonic stress at plate boundaries, the above correlation suggests that the regional difference in the level of tectonic stress is at least partially responsible for the regional variation of volcanic rock series.

SUBDUCTION ZONE SEISMICITY AND STRESS IN SLABS

M. S. Vassiliou
B. H. Hager
D. L. Anderson
A. Raefsky
(all at: Seismological Laboratory 252-21, California Institute of Technology, Pasadena CA 91125)

Histograms of log N (# earthquakes) plotted against depth (NOAA & PDE catalogs, $m_b > 4$, 1964-1980) have the following features: a roughly linear decay down to 250-300 km., followed by either (1) a complete cessation or (2) a minimal level in turn followed by a resurgence. There is a cessation beyond 650-700 km, perhaps associated with the 670 km seismic discontinuity. The degree to which the initial decay is linear varies among regions, as does the slope of the decay. Slopes correlate only weakly with subduction parameters such as convergence rate.

A model of a viscous slab sinking vertically in a less viscous medium with a rigid bottom boundary at 670 km yields a slab stress magnitude which decreases linearly with depth down to ~ 250 km, and then increases. This simple model, with an assumption that N varies exponentially as the stress, can explain the important features of the seismicity curves. More complex models including dipping slabs and various boundary conditions differ in details, but there is a broad class of models which preserves the essential characteristics mentioned above.

1. 1981 Fall Meeting

2. VASS049504

3. Corresponding address:

   M.S. Vassiliou
   Caltech 252-21
   Pasadena, CA 91125
   213-356-6912

4. T (Tectonophysics)

5. none

6. O (oral)

7. none

8. a. Bill to:
      Seismological Lab 252-21
      Calif. Inst. of Tech.
      Pasadena, CA 91125

   b. P.O.

   c. Student rate applicable

9. C (Contributed)

A DYNAMICALLY CONSISTENT CALCULATION OF GEOID ANOMALIES IN A VISCOUS PLANET WITH IMPLICATIONS FOR GEOID INTERPRETATION

Mark A. Richards
Bradford H. Hager (Both at: Seismological Laboratory, Caltech, Pasadena, CA 91125)
(Sponsor: B. H. Hager)

The Earth and other terrestrial planets are better approximated as viscous than as rigid spheres. Interior density contrasts cause flow and stresses which lead to deformation of the outer surface and interior boundaries. These deformed surfaces cause additional geoid anomalies which must also be considered in evaluating the total geoid anomaly resulting from an interior density contrast.

We calculate self-consistent geoid anomalies for density contrasts in a viscous self-gravitating sphere as a function of spherical harmonic degree ℓ. Free-slip boundary conditions are applied at the core-mantle boundary and no-slip boundary conditions are applied at the surface. Additional mass anomalies arise when the boundaries are deformed by the normal stresses. For a uniform mantle, deformation of the boundaries leads to a larger contribution to the total geoid anomaly than the density contrast itself for all ℓ, resulting in negative geoid anomalies for positive density contrasts. For intermediate ℓ, geoid anomalies from density contrasts in the lower mantle are an order of magnitude larger than those obtained for a rigid Earth, reopening the question of the maximum depth of density anomalies which can generate the observed geoid.

For a planet with chemical or viscosity layering the behavior is more complicated. The sign and magnitude of the geoid anomaly depend upon the viscosity structure, wavelength, and depth of the density anomaly. We conclude that interpretation of geoid data in terms of density contrasts requires gross assumptions about the mantle's rheology and composition.

1. 1981 Fall Meeting
2. HAGE038920 (Sponsor)
3. Corresponding address:

   Mark A. Richards
   California Institute
   of Technology, 252-21
   Pasadena, CA 91125
   213-356-6974
4. T(Tectonophysics)
5. None
6. O (oral)
7. 0%
8. a. Bill to:
      Seismological Lab 252-21
      Calif. Inst. of Tech.
      Pasadena, CA 91125

   b. P.O. 66-550503

   c. Student rate applicable
9. C (Contributed)

THE OCT. 1980 EARTHQUAKE SEQUENCE IN A SEISMIC GAP NEAR THE LOYALTY IS., NEW HEBRIDES

John Vidale (Seismological Laboratory, California Institute of Technology, Pasadena, California 91125)
Hiroo Kanamori (Same)

Four large earthquakes occurred in a seismic gap of category 2 (McCann et al., 1979) near the Loyalty Is. in the New Hebrides. At 3:25 on Oct. 24, 1980, an event with M_S=6.7 initiated the sequence. Three events, M_S=6.7, 7.2, and 6.5 followed this event on the next day.

We investigated this sequence by using the PDE data, first-motion data from WWSSN records, and long-period surface waves recorded by IDA, SRO, and ASRO stations. The first-motion data constrained one of the nodal planes. With this constraint, inversion of Rayleigh and Love-wave spectra at 256 seconds determined the other nodal plane. The mechanisms of all four events are almost pure thrust on a plane dipping 20° and striking parallel to the local strike of the New Hebrides trench. The first-day aftershocks indicate an initial rupture zone of about 2,000 km^2 which is consistant with the estimated seismic moment of 3×10^{27} dyne-cm. During the next two days, the aftershock activity expanded to an area of 10,000 to 20,000 km^2 in the directions both along and perpendicular to the trench. This pattern suggests that the initial rupture zone represents a zone of increased strength (i.e. asperity), and the stress change due to failure of this asperity subsequently migrated outward. During the 2 year period before the main event, seismicity in the initial rupture zone had been very low except near the point where the main shock sequence initiated. A very tight clustering of activity occurred there. This pattern indicates gradual stress concentration near the asperity which finally failed during the main-shock sequence.

Since the physical condition of the fault zone is expected to persist in time, the present results would help predict the behavior of this gap during the next sequence.

1. 1981 Fall Meeting

2. VIDA 206316

3. Corresponding address:

   John Vidale
   Caltech 252-21
   Pasadena, CA 91125
   213-356-6976

4. S (Seismology)

5. None

6. O (oral)

7. none

8. a. Bill to:
      Seismological Lab 252-21
      Calif. Inst. of Tech.
      Pasadena, CA 91125

   b. P.O.

   c. Student rate applicable

9. C (Contributed)

AN ARRAY STUDY OF THE UPPER MANTLE BENEATH WESTERN MEXICO

Marianne C. Walck (Seismological Laboratory, California Institute of Technology, Pasadena, California 91125)
Don L. Anderson

The Caltech - USGS Southern California Seismic Network (SCARLET) is favorably located to record short-period P-wave arrivals from earthquakes in Mexico and central America (Az = 330±15°, $\Delta < 40^{\circ}$) which have traversed upper mantle paths beneath tectonically active regions. The large number of moderate ($5.0 < M_b < 6.0$) earthquakes occurring in this area since 1977 provide an excellent data base for the investigation of the Gulf of California's upper mantle velocity structure. Record sections have been constructed for 29 events at distances of 8°-40°; each section has a station spacing of ~10 km and extends 4.5° in distance. Arrivals from the triplications associated with the two major upper mantle discontinuities are clearly visible for many events. Times of all prominant phases were used in direct determinations of $dT/d\Delta$ for each earthquake. Because of severe near-receiver structural effects, we first applied station corrections derived from relative arrival times of distant ($\Delta > 30^{\circ}$) events along the same azimuth. The resulting $dT/d\Delta$ profile has little scatter. Abundant data between 18°and 25° strongly constrain the velocity gradient between the '400 km' and '650 km' discontinuities; in this range the data is similar to that of King and Calcagnile's (1976) model for northern Eurasia.

1. 1981 Fall Meeting
2. WALC200975
3. Corresponding address:

   Marianne C. Walck
   Caltech 252-21
   Pasadena, CA 91125
   213-356-6971
4. S (Seismology)
5. none
6. O (oral)
7. none
8. a. Bill to:
      Seismological Lab 252-21
      Calif. Inst. of Tech.
      Pasadena, CA 91125

   b. P.O. 66-550486

   c. Student rate applicable
9. C (Contributed)